

# Journal of Visualized Experiments

## Preparation of Graphene-Supported Microwell Liquid Cells for In Situ Transmission Electron Microscopy --Manuscript Draft--

<b>Article Type:</b>	Invited Methods Article - JoVE Produced Video
<b>Manuscript Number:</b>	JoVE59751R1
<b>Full Title:</b>	Preparation of Graphene-Supported Microwell Liquid Cells for In Situ Transmission Electron Microscopy
<b>Keywords:</b>	liquid cell transmission electron microscopy; in situ; nanoparticles; graphene; growth kinetics; precursor solutions; gold
<b>Corresponding Author:</b>	Andreas Hutzler, Dr.-Ing. Friedrich-Alexander-Universitat Erlangen-Nurnberg Erlangen, Bavaria GERMANY
<b>Corresponding Author's Institution:</b>	Friedrich-Alexander-Universitat Erlangen-Nurnberg
<b>Corresponding Author E-Mail:</b>	Andreas.Hutzler@leb.eei.uni-erlangen.de
<b>Order of Authors:</b>	Andreas Hutzler, Dr.-Ing. Birk Fritsch Michael P. M. Jank Robert Branscheid Erdmann Spiecker Martin März
<b>Additional Information:</b>	
<b>Question</b>	<b>Response</b>
Please indicate whether this article will be Standard Access or Open Access.	Open Access (US\$4,200)
Please indicate the <b>city, state/province, and country</b> where this article will be <b>filmed</b> . Please do not use abbreviations.	Erlangen, Bavaria, Germany

**TITLE:**

Preparation of Graphene-Supported Microwell Liquid Cells for In Situ Transmission Electron Microscopy

**AUTHORS & AFFILIATIONS:**

Andreas Hutzler<sup>\*,1</sup>, Birk Fritsch<sup>\*,1</sup>, Michael P. M. Jank<sup>2</sup>, Robert Branscheid<sup>3</sup>, Erdmann Spiecker<sup>3</sup>, Martin März<sup>1,2,4</sup>

\*These authors share equal contribution.

<sup>1</sup>Electron Devices (LEB), Department of Electrical, Electronic and Communication Engineering, Friedrich-Alexander University Erlangen-Nürnberg, Erlangen, Germany

<sup>2</sup>Fraunhofer Institute for Integrated Systems and Device Technology (IISB), Erlangen, Germany

<sup>3</sup>Institute of Micro- and Nanostructure Research (IMN) and Center for Nanoanalysis and Electron Microscopy (CENEM), Department of Materials Science and Engineering, Friedrich-Alexander University Erlangen-Nürnberg, Erlangen, Germany

<sup>4</sup>Power Electronics (LEE), Department of Electrical, Electronic and Communication Engineering, Friedrich-Alexander University Erlangen-Nürnberg, Nuremberg, Germany

Corresponding Author:

Andreas Hutzler

Email Address: [andreas.hutzler@leb.eei.uni-erlangen.de](mailto:andreas.hutzler@leb.eei.uni-erlangen.de)

Email Addresses of Co-authors:

Birk Fritsch ([birk.fritsch@leb.eei.uni-erlangen.de](mailto:birk.fritsch@leb.eei.uni-erlangen.de))

Michael P. M. Jank ([michael.jank@iisb.fraunhofer.de](mailto:michael.jank@iisb.fraunhofer.de))

Robert Branscheid ([robert.branscheid@fau.de](mailto:robert.branscheid@fau.de))

Erdmann Spiecker ([erdmann.spiecker@fau.de](mailto:erdmann.spiecker@fau.de))

Martin März ([martin.maerz@iisb.fraunhofer.de](mailto:martin.maerz@iisb.fraunhofer.de))

**KEYWORDS:**

liquid cell, in situ TEM, nanoparticles, synthesis, etching, growth, gold, kinetics, graphene, dendrite, single particle tracking

**SHORT ABSTRACT:**

A protocol for preparation of graphene-supported microwell liquid cells for in situ electron microscopy of gold nanocrystals from HAuCl<sub>4</sub> precursor solution is presented. Furthermore, an analysis routine is presented to quantify observed etching and growth dynamics.

**LONG ABSTRACT:**

The fabrication and preparation of graphene-supported microwell liquid cells (GSMLCs) for in situ electron microscopy is presented in a stepwise protocol. The versatility of the GSMLCs is demonstrated in the context of a study about etching and growth dynamics of gold nanostructures from a HAuCl<sub>4</sub> precursor solution. GSMLCs combine the advantages of conventional silicon- and graphene-based liquid cells by offering reproducible well depths together with facile cell manufacturing and handling of the specimen under investigation. The

GSMLCs are fabricated on a single silicon substrate which drastically reduces the complexity of the manufacturing process compared to two-wafer-based liquid cell designs. Here, no bonding or alignment process steps are required. Furthermore, the enclosed liquid volume can be tailored to the respective experimental requirements by simply adjusting the thickness of a silicon nitride layer. This enables a significant reduction of window bulging in the electron microscope vacuum. Finally, a state-of-the-art quantitative evaluation of single particle tracking and dendrite formation in liquid cell experiments using only open source software is presented.

## INTRODUCTION:

Modern materials science, chemistry and cell biology require a deep understanding of underlying dynamic processes and effects at the sub-micron scale. Despite the power of advanced optical microscopy techniques such as stimulated-emission-depletion fluorescence microscopy<sup>1</sup>, direct imaging techniques to access detailed morphologies require electron microscopy. In particular, in situ (scanning) transmission electron microscopy (S)TEM has been shown to illuminate valuable insights into process dynamics by encapsulating liquids in dedicated, vacuum-tight cells<sup>2</sup>. Various experiments such as quantitative investigations of nanostructure formation kinetics and thermodynamics<sup>3–6</sup>, imaging of biological specimens<sup>7–10</sup> and studies of energy storage-related mechanisms<sup>11,12</sup> along with comprehensive studies of corrosion process dynamics<sup>13</sup> or nanobubble physics<sup>14–16</sup> have unraveled many phenomena using (S)TEM that were not accessible using standard microscopy techniques.

During the last decade, two major approaches to realize in situ liquid cell TEM (LCTEM) have been established. In the first approach, the liquid is encapsulated in a cavity between two Si<sub>3</sub>N<sub>4</sub> membranes produced via Si process technology<sup>17</sup>, whereas in the second, small liquid pockets are formed between two graphene or graphene oxide sheets<sup>10,18</sup>. The handling of both silicon-based liquid cells (SiLCs) and graphene-based liquid cells (GLCs) has been demonstrated<sup>19–21</sup>. Although both approaches have undergone significant improvements<sup>22–25</sup>, they still lack in the combination of the respective advantages. In general, a tradeoff exists between encapsulating the sample in often undefined graphene pockets with a small liquid volume that enables high-resolution imaging<sup>18</sup>, and well defined cell volumes resulting in thicker membranes and liquid layers, which provide an environment closer to the natural situation in bulk liquid<sup>26</sup> at the expense of resolution<sup>2</sup>. Furthermore, some experiments depend on a liquid flow<sup>26,27</sup> which has only been realized in SiLC architectures and requires a dedicated TEM holder<sup>28</sup>.

Here, we present the fabrication and handling of a liquid cell approach for high-performance in situ LCTEM via static graphene-supported microwell liquid cells (GSMLCs) for TEM analyses. A sketch of the GSMLC is presented in **Figure 1**. GSMLCs have proven to be capable of enabling in situ high-resolution transmission electron microscopy (HRTEM) results<sup>6</sup> and are also feasible for in situ scanning electron microscopy<sup>29</sup>. Their Si technology-based frame allows for mass production of reproducibly shaped cells with tailored liquid thickness and extra-thin membranes from a single wafer. The graphene membrane covering these cells also mitigates electron beam-induced perturbations<sup>8,30,31</sup> since the electron beam passes through the top graphene membrane first. The flat topography of the cells allow for complementary analysis methods such as energy-dispersive X-ray spectroscopy (EDXS)<sup>6</sup> without any shadowing effects arising from the liquid cell

itself, enabling a variety of high-quality in situ liquid cell electron microscopy experiments.

## **PROTOCOL:**

### **1. Fabrication of microwell-based liquid cell templates**

1.1. Remove organic residues and native oxide layers from a 175  $\mu\text{m}$  thick, single crystalline, boron-doped (1 – 30)  $\Omega\text{cm}$ , 100 mm diameter (100) silicon wafer. Apply an oxidation step with  $\text{H}_2\text{O}_2$  and TMAH, followed by a HF dip in 1 – 5% HF solution.

1.2. Thermally oxidize the wafer in a dry oxygen atmosphere at 800  $^\circ\text{C}$  to grow an oxide layer with a thickness of 11 nm (**Figure 2a**). 3% Dichlorethene (DCE) is used to bind metallic contamination.

1.3. Deposit a stoichiometric  $\text{Si}_3\text{N}_4$  layer via low-pressure chemical vapor deposition (LPCVD). The  $\text{Si}_3\text{N}_4$  layer thickness defines the well depth. Choose a value suited for the planned experiment (e.g., 500 nm) (**Figure 2 b**).

1.4. Define the lateral well geometry by structuring the front side via photolithography and reactive ion etching (RIE) (**Figure 2c**). Suitable dimensions are for example circular structures with 2.5  $\mu\text{m}$  radius arranged in hexagonal arrays. Choose the well distance carefully (for example, 5  $\mu\text{m}$ ), to avoid instabilities in the structure.

1.5. Deposit another 20 nm of stoichiometric  $\text{Si}_3\text{N}_4$  by LPCVD, which forms the bottom membrane of the liquid cell (**Figure 2d**). Follow the procedure described above (see step 1.3).

1.6. Use a second photolithography/RIE step to structure the backside which later defines the geometrical dimensions of the LC and its TEM windows (**Figure 2e**).

1.7. Via bulk-micromachining in 20% KOH at 60  $^\circ\text{C}$ , remove the Si in the predefined area and create a free-standing  $\text{Si}_3\text{N}_4$  membrane (**Figure 2f**).

1.8. Remove residual metal ions in a final cleaning step with 10% HCl solution and deionized (DI) water.

### **2. Transfer of graphene onto TEM grids**

2.1 Wet the tissue on which the commercially acquired few-layer (6 – 8) CVD-graphene on PMMA is placed. Immerse the PMMA-coated graphene in a Petri dish filled with DI water (**Figure 3a**).

2.2 Place the graphene layer on a filter paper and cut it into pieces suitable to cover all fabricated wells (e.g., 4  $\text{mm}^2$ ) (**Figure 3b**).



2.3 Re-immerse the cut pieces into the Petri dish (**Figure 3c**).

2.4 Use a TEM grid coated with a support layer of holey carbon to fish the produced pieces out of the DI water. To do so, carefully dive the grid into the water and catch the graphene floating on the surface. Hold the grid with anti-capillary tweezers (**Figure 3d,e**).

NOTE: Take care that the graphene side of the graphene-PMMA stack stays on top during the whole procedure. Otherwise, the subsequent PMMA-removal will lift-off the graphene layer.

2.5 Let the sheets dry for a few hours.

2.6 Remove the PMMA protection layer in an acetone bath for 30 min and consecutively add further cleaning steps by immersing in ethanol and DI water without drying the sample in between. Use a flat vessel (e.g., a Petri dish) to simplify the specimen transfer afterwards.

2.7 Dry the sample afterwards for 30 min at ambient conditions.

### 3. Specimen preparation

3.1 Prepare the specimen for incorporation in the GSMLC. To do so, prepare a 1 mM stock solution by solving 196.915 mg of  $\text{HAuCl}_4 \cdot 3\text{H}_2\text{O}$  crystals in 0.5 L of DI water.

3.1. Take the desired amount of specimen from the stock solution. Here, 0.1  $\mu\text{L}$  is applied. This can be done by using a syringe or an Eppendorf pipette.

### 4. GSMLC loading

4.1. Rinse the fabricated liquid cell template with acetone and ethanol.

4.2. Apply an ambient  $\text{O}_2/\text{N}_2$  (20%/80%) plasma for 5 min to enhance the wettability of the membrane.

4.3. Dispense 0.1  $\mu\text{L}$  of specimen solution on the template or the graphene layer. Ensure a smooth working procedure to minimize changes in concentration due to evaporation.

4.4. Place the TEM grid onto the micro-patterned  $\text{Si}_3\text{N}_4$  layer with the graphene facing the template. Press the graphene-coated TEM grid onto the template. Be careful not to destroy the bottom  $\text{Si}_3\text{N}_4$  membrane.

4.5. Remove excess solution with a tissue to accelerate the cell drying and thus mitigate concentration changes (**Figure 4a**). After approx. 2 – 3 min, the graphene- $\text{Si}_3\text{N}_4$  van-der-Waals interaction sufficiently seals the liquid cell (**Figure 4b**). Alternatively, leave the cell to dry out completely without removing the excess solution. The latter offers a higher success rate in the cell processing. However, evaporation-based concentration changes in the specimen solution are

expected to be more severe when using this approach.

NOTE: The successful drying process can be verified with a contrast change in the periphery (compare **Figure 4a,b**).

4.6. Carefully remove the TEM grid with a tweezer by pushing a tweezer tip between the grid and the GSMLC frame.

NOTE: Rash movements might break the underlying membrane. To reduce shear force damage, start from the grid site parallel to the smaller window edge.

4.7. Check, whether at least one membrane of the GSMLC is still intact via optical microscopy (**Figure 4c**). If all membranes were broken, LCTEM would be impossible.

## 5. TEM Imaging and video analysis

5.1. Load the sample to a (S)TEM directly after preparation using a standard TEM holder.

NOTE: As it is reported for GLCs<sup>19</sup>, GSMLCs can dry out over time. Therefore, the time between loading and imaging should be minimized.

5.2. Image the sample with a suitable imaging technique, depending on both the sample and microscope. Here, a (S)TEM device operated at an acceleration voltage of 300 kV is utilized. Use a low dose to minimize beam-induced artifacts and a short exposure time to avoid movement-related blurring<sup>32</sup>. In case of long-term experiments, block the beam to reduce radiation damage.

NOTE: Due to a better temporal resolution, TEM is to be preferred over STEM for kinetic analyses<sup>32</sup> and reduced ion reduction<sup>33</sup>. STEM, however, is preferred for investigation into thick liquid layers and high-Z elements due to its higher spatial resolution in thick specimens<sup>32,33</sup>.

### 5.3. Image segmentation method

5.3.1. Use a suitable image processing platform to extract features of interest. For particle tracking and analysis, use the open source ImageJ-distribution FIJI<sup>34</sup>.

5.3.2. Utilize the **Analyze Particles** function to gain precise information (projected area, barycenter) of every particle in each frame.

NOTE: This function requires binary images.

5.3.3. Connect the particles between the frames with the help of the plugin TrackMate<sup>35</sup>. By default, TrackMate is searching for bright particles on a dark background, so invert the images (in the case of BF-TEM) before starting TrackMate.

5.3.4. Combine the results of TrackMate and **Analyze Particles** with a suitable script utilizing the Python-based open source ecosystem SciPy<sup>36,37</sup>.

5.3.5. Use FIJI to extract the precise contours of more complex structures such as dendrites. Here, Analyze Particles can be applied, as well (see inset of **Figure 6a**).

NOTE: It might be feasible to analyze features of interest manually.

#### REPRESENTATIVE RESULTS:

After loading of the cell, a successful graphene transfer is indicated by a differently shaded appearance on the wells under an optical microscope. This is visible, for example, in the right membrane of **Figure 3c**. As mentioned, it is crucial to carefully remove the TEM-grid in order to not break the thin Si<sub>3</sub>N<sub>4</sub> layer. In case of a broken membrane, lucent and curved residuals are clearly visible in the optical microscope, as shown in the left two membranes of **Figure 3c**. Due to the multiple viewing areas in the utilized GSMLC design, the cell can be used as long as at least one membrane is intact. Broken membranes can be used for TEM alignment without exposing the specimen to the electron beam.

A successful encapsulation of the specimen solution can be verified during electron microscopy. **Figure 5** presents individual micrographs of **Supplementary Video 1**, where the dissolution of an ensemble of nanoparticles and the growth of a dendritic structure is statistically evaluated in a GSMLC. Besides the drift-induced movement of the image, minor individual orthogonal particle movements are visible, indicating that particles in solution are present. Furthermore, the prevalence of particle dissolution proves that a wet-chemical reaction is present which would not be possible without a successful liquid enclosing. Other typical indications for enclosed liquids are beam-induced bubble formation<sup>19</sup> or particle motion. The presence of Au particles in graphene-featured cells alone does not conclusively indicate a liquid environment, since the particles could also stem from the graphene-induced reduction of HAuCl<sub>4</sub><sup>38</sup>. A quantification of the oxygen peaks of the enclosed liquid via electron energy loss spectroscopy (EELS) can also be performed to verify a liquid environment<sup>39</sup>.

In order to gain insights into particle growth and dissolution kinetics, it is important to investigate each particle individually rather than to analyze the development of average parameters<sup>40</sup>. It is also crucial to exclude particles at the frame edges that are only partially captured by the camera because drift effect-related position changes of such particles might be mistaken as growth or dissolution processes. Etching is believed to be caused by oxidative species generated by electron beam-induced radiolysis<sup>41</sup>. In order to yield sufficient statistics, computational single particle tracking is required. By estimating the growth exponent  $\alpha$  of the equivalent radius variation of individual particles over time, information of the underlying reaction kinetics can be obtained. To do so, it is possible to introduce an equivalent radius based on the projected particle area, even if not all particles are completely spherical<sup>6,42</sup>. **Figure 5b** shows the tracking of equivalent radii over time for six representative particles which are highlighted in **Figure 5a**. **Figure 5c** shows the distribution of  $\alpha$  based on 73 dissolving particles from the present study. Only particles where an allometric model explains the radius decline to at least 75% (adjusted coefficient of

determination) are regarded.

Furthermore, a dendrite structure emerges rapidly after about 42 s in the same well depicted in **Figure 6a**. Dendrite formation is another typical, well documented process in liquid cells<sup>43,44</sup>. To quantify dendrite growth, the structural outlines (see inset in **Figure 6a**) are analyzed. The evolution of tip radius and velocity over time (see **Figure 6b,c**) reveals the expected hyperbolic relationship<sup>45</sup> (**Figure 6d**). Dendrite growth is caused by local supersaturation of Au-ions due to the aforementioned particle etching. In **Figure 5a**, it is clearly visible that particles are still dissolving whilst the oversaturated system relaxes into dendrite growth. This may be caused by local concentration variations in both the Au-ions and the oxidative species as a result of the high viscosity of the liquid in the GSMLC which has been observed before<sup>6</sup>. A detailed discussion of this phenomenon, however, is beyond the scope of this work.

## FIGURE & TABLE LEGENDS:

**Figure 1: Sketch of a GSMLC: Schematics of the structure of a graphene-supported microwell liquid cell.** Reprinted from <https://pubs.acs.org/doi/abs/10.1021/acs.nanolett.8b03388><sup>6</sup>. Further permissions are to be directed to the American Chemical Society (ACS).

**Figure 2: Fabrication of GSMLC-frames.** The fabrication process of GSMLC-frames is schematically sketched. **(a)** Oxidation of Si wafer after cleaning. **(b)** LPCVD of Si<sub>3</sub>N<sub>4</sub>. **(c)** Front side Si<sub>3</sub>N<sub>4</sub> patterning by photolithography and RIE to define the cell volume. **(d)** Deposition of Si<sub>3</sub>N<sub>4</sub> to form the bottom cell window. **(e)** Back-side lithography and RIE. **(f)** Bulk micromachining with KOH to create a freestanding Si<sub>3</sub>N<sub>4</sub> membrane containing microwells.

**Figure 3: Transfer of few-layer CVD-graphene with PMMA protection layer onto a TEM-grid.** The transfer of few-layer CVD-graphene on PMMA onto the top of a holey carbon-coated TEM-grid is displayed. **(a)** Immersion of the few-layer CVD graphene on PMMA in a Petri dish filled with DI water. **(b)** Transferred graphene/PMMA stack on a filter paper is cut into pieces suitable to cover the GSMLC-frames. **(c)** Re-immersion of a cut graphene/PMMA piece. **(d)** Transfer of the graphene/PMMA layer onto a holey carbon-coated TEM grid **(e)** Graphene/PMMA stack after a successful transfer.

**Figure 4: Removal of the top TEM grid.** The drying process of a loaded GSMLC is documented with the help of an optical microscope. **(a)** A graphene-coated TEM grid is placed on top of the GSMLC directly after loading. The graphene layer is visible as turquoise rectangle covering all three viewing areas. Its outlines are roughly sketched by the black rectangle. **(b)** An almost completely adhered membrane is visible by the contrast change between the wet (dark, compare with (a)) and the adhered area (turquoise) after approximately two minutes. **(c)** A GSMLC after the lift-off of the TEM grid is shown, revealing two broken membranes (left and middle), and one membrane with successfully loaded and sealed microwells (right).

**Figure 5: Representative development of nanoparticle radii.** The radius development of 183 individual particles has been tracked. **(a)** Image sequence taken from **Supplementary Video 1**.

Six representative particles are highlighted. The colored circles correspond to the obtained equivalent radius. **(b)** Logarithmic plot of the particle radii. **(c)** The histogram of 73 particles where a negative allometric exponent  $\alpha$  has been determined using an automated routine.

**Figure 6: Dendrite dynamics: The tip radius of five dendrite branches is analyzed.** Error bars account for the respective standard deviation. **(a)** Image sequence taken from **Supplementary Video 1** showing the emerging dendrite, which is visible after about 42 s. The inset in the right image shows the evolving dendrite contours. Here, the pink outlines correspond to 42.09 s, red to 42.7 s, and purple to 43.3 s. **(b)** Development of the (averaged) tip radius over time. **(c)** The mean tip velocity plotted over time. **(d)** The averaged tip radius logarithmically plotted against the averaged tip velocity, revealing a hyperbolic dependency (orange curve).

**Figure 7: SEM Image of a loaded GSMLC: A representative SEM image acquired in HAADF STEM mode in an SEM of a loaded GSMLC at low acceleration voltage (29 kV) is displayed.** Besides the prominent 5  $\mu\text{m}$  wide microwells, two partially overlapping circular holey carbon grids (2  $\mu\text{m}$  diameter) stemming from the graphene transfer elucidated above is visible. The first carbon grid stems from an unsuccessful graphene transfer. It is clearly visible that the membrane shading stays mostly constant over the well region, but slightly darkens towards the well center. This accounts for weak, negative bulging.

**Supplementary Video 1: In situ video showing representative results of a liquid cell bright field TEM study of etching of Au nanoparticles and subsequent growth of a dendrite structure caused by supersaturation of the surrounding specimen solution.**

## DISCUSSION:

In contrast to commercially available liquid cells, custom-made GSMLCs have the advantage that they can be designed to fit into readily available TEM holders and do not require an expensive, dedicated liquid cell TEM holder.

The GSMLC architecture demonstrated here combines aspects of SiLCs and GLCs that could potentially lead to unique advantages. On the one hand, SiLCs allow for a precise determination of cell position and shape, but require relatively thick  $\text{Si}_3\text{N}_4$  membranes to reduce bulging effects while ultimately reducing the achievable resolution. GLCs, on the other hand, exhibit exceptionally thin membrane walls consisting of graphene, yet suffer from random pocket sizes and positions. By combining these two membrane approaches via GSMLCs, the resolution limitation caused by the cell boundaries<sup>33</sup> can be bypassed. As the well structure is fabricated directly into the  $\text{Si}_3\text{N}_4$  layer, the actual  $\text{Si}_3\text{N}_4$  membrane can be constructed even smaller than in SiLCs, simplifying HRTEM analyses which has already been demonstrated in GSMLCs<sup>6</sup>. Still, it should be noted that HRTEM in general is possible with SiLCs as well<sup>46</sup>. Moreover, large viewing areas can be realized without severe window bulging due to the small membrane areas of the individual specimen chambers. Thereby, bulging-related thickness increase<sup>33</sup> can be ruled out to a large extent, as shown by Dukes et al.<sup>47</sup>. This is demonstrated in **Figure 7**, where a representative high-angle annular dark field (HAADF) STEM image of a loaded GSMLC is

displayed. This image was acquired using a Dual-beam system. Since the image brightness acquired in this setup is directly related to the specimen thickness, it is clearly visible that the sealed microwells exhibit only small negative bulging. Kelly et al.<sup>24</sup> have demonstrated that the negative bulging and partial well drying visible in **Figure 7** depends on the well diameter. Reducing the well diameter is therefore a feasible approach to homogenize the liquid thickness even further.

Due to the equilibrium pocket shape of GLCs, the liquid thickness is also strongly site-dependent<sup>33</sup>. SiLCs follow the design of two membranes stemming from different Si wafers. By replacing the top Si<sub>3</sub>N<sub>4</sub> membrane with graphene, liquid-cell fabrication is simplified. This means that possible delamination of two bonded Si-wafers during the subsequent wet etching steps can be avoided and the alignment of two wafer pieces during the cell loading is omitted. The flat surface on one side of this cell architecture enables complementary in situ analysis methods such as EDXS analysis of the specimen<sup>6</sup>, which is restricted in conventional SiLC architectures by shadowing effects at steep Si edges<sup>48</sup>.

Sealing prepatterned microwells with graphene on both the bottom and top well site has been demonstrated before<sup>24,25</sup>. Applying two graphene membranes may enhance the achievable resolution. A twofold graphene transfer, however, would complicate the preparation process further; especially since this has proven to be the most sensitive preparation step (see below). Furthermore, the above discussed membrane bulging is expected to be even more critical in case of two graphene membranes, because graphene is much more flexible than a Si<sub>3</sub>N<sub>4</sub> layer. In those architectures, the microwells were constructed using sequential focused ion beam (FIB) milling. While this approach has proven to yield high-quality results, FIB milling is complicated and expensive cell production technique. Utilizing massively parallel single-shot patterning techniques that are already standard in today's semiconductor industry such as nanoimprint- or photolithography, however, has the major advantage of being fast, cheap and scalable for mass production.

It should be noted that the approach presented here does not allow for liquid flow operation, which is achievable by other designs<sup>28</sup>. Since the loading and liquid volume are comparable for GSMLCs and GLCs, a contamination of high vacuum due to rupture of the membrane can be avoided<sup>19</sup>. This eliminates the need for a cumbersome seal check. Though the advantages of SiLCs and GLCs have been combined, the disadvantages of both approaches are still present in GSMLCs. The fabrication of the cells requires a clean room infrastructure for silicon technology, which is not necessarily present in TEM laboratories. In addition, the liquid loading is not trivial. It requires a dedicated training, similar to graphene cells. This, however, is also true for commercially available systems. Here, the most sensitive preparation step is the TEM-grid removal after the graphene transfer because rash movements or jittering is likely to break the Si<sub>3</sub>N<sub>4</sub> layer. The redundant membrane windows, however, enhance the chances of preserving at least one membrane area. As a consequence, the yield (amount of operable GSMLC chips) achieved by a trained experimenter is three out of four<sup>6</sup>, and thus exceeds the one achieved with graphene-based cells (one to two out of four)<sup>19</sup>.

As with GLCs, the liquid encapsulation in GSMLCs is based on van-der-Waals interactions<sup>18</sup>. Consequently, interface contamination could lower the success rate in processing of GSMLCs<sup>19</sup>. Furthermore, depending on the Hamaker constant of the to-be-encapsulated liquid phase, the wetting characteristics during the loading procedure (and thus the achievable yield) may differ<sup>49</sup> and therefore the preparation can be complicated. Our experience shows that this is the case if, for example, amphiphilic species are present.

The GSMLC architecture enables flexible configuration of well-depths, allowing for adaptation to various experimental prerequisites. Moreover, the architecture is suitable for electron tomography investigations over a broad tilt-angle range of  $\pm 75^\circ$ , which would also allow for in situ electron tomography<sup>50</sup>. Therefore, in situ and post mortem tomography of specimen in liquid could also be established with GSMLCs.

#### ACKNOWLEDGMENTS:

We thank Tilo Schmutzler for the preparation of the  $\text{HAuCl}_4$  solution. Furthermore, we thank R. Christian Martens for proof reading. Financial support by the German Research Foundation (DFG) via the Research Training Group GRK 1896 “In situ microscopy with electrons, X-rays and scanning probes” and through the Cluster of Excellence EXC 315/2 EAM “Engineering of Advanced Materials” is gratefully acknowledged.

#### DISCLOSURES:

We have nothing to disclose.

#### References

1. Hell, S.W., Wichmann, J. Breaking the diffraction resolution limit by stimulated emission: stimulated-emission-depletion fluorescence microscopy. *Optics Letters*. **19** (11), 780, 10.1364/OL.19.000780 (1994).
2. Ross, F.M. Liquid Cell Electron Microscopy. Cambridge University Press (2016).
3. Alloyeau, D. et al. Unravelling kinetic and thermodynamic effects on the growth of gold nanoplates by liquid transmission electron microscopy. *Nano letters*. **15** (4), 2574–2581, 10.1021/acs.nanolett.5b00140 (2015).
4. Tao, J., Nielsen, M.H., Yoreo, J.J. de Nucleation and phase transformation pathways in electrolyte solutions investigated by in situ microscopy techniques. *Current Opinion in Colloid & Interface Science*. **34**, 74–88, 10.1016/j.cocis.2018.04.002 (2018).
5. Jin, B., Sushko, M.L., Liu, Z., Jin, C., Tang, R. In Situ Liquid Cell TEM Reveals Bridge-Induced Contact and Fusion of Au Nanocrystals in Aqueous Solution. *Nano letters*. **18** (10), 6551–6556, 10.1021/acs.nanolett.8b03139 (2018).
6. Hutzler, A. et al. Unravelling the mechanisms of gold-silver core-shell nanostructure formation by in situ TEM using an advanced liquid cell design. *Nano letters*. **18** (11), 7222–7229, 10.1021/acs.nanolett.8b03388 (2018).
7. Moser, T.H. et al. The role of electron irradiation history in liquid cell transmission electron microscopy. *Science advances*. **4** (4), eaaq1202, 10.1126/sciadv.aaq1202 (2018).
8. Keskin, S., Jonge, N. de Reduced Radiation Damage in Transmission Electron Microscopy of Proteins in Graphene Liquid Cells. *Nano letters*, **18** (12), 7435–7440,

10.1021/acs.nanolett.8b02490 (2018).

9. Firlar, E. et al. Investigation of the magnetosome biomineralization in magnetotactic bacteria using graphene liquid cell - transmission electron microscopy. *Nanoscale*. **11** (2), 698–705, 10.1039/c8nr08647h (2019).

10. Mohanty, N., Fahrenholtz, M., Nagaraja, A., Boyle, D., Berry, V. Impermeable graphenic encasement of bacteria. *Nano letters*. **11** (3), 1270–1275, 10.1021/nl104292k (2011).

11. Gu, M. et al. Demonstration of an electrochemical liquid cell for operando transmission electron microscopy observation of the lithiation/delithiation behavior of Si nanowire battery anodes. *Nano letters*. **13** (12), 6106–6112, 10.1021/nl403402q (2013).

12. Lutz, L. et al. Operando Monitoring of the Solution-Mediated Discharge and Charge Processes in a Na-O<sub>2</sub> Battery Using Liquid-Electrochemical Transmission Electron Microscopy. *Nano letters*. **18** (2), 1280–1289, 10.1021/acs.nanolett.7b04937 (2018).

13. Chee, S.W. et al. Studying localized corrosion using liquid cell transmission electron microscopy. *Chemical communications* (Cambridge, England). **51** (1), 168–171, 10.1039/c4cc06443g (2015).

14. Grogan, J.M., Schneider, N.M., Ross, F.M., Bau, H.H. Bubble and pattern formation in liquid induced by an electron beam. *Nano letters*. **14** (1), 359–364, 10.1021/nl404169a (2014).

15. Tomo, Y., Li, Q.-Y., Ikuta, T., Takata, Y., Takahashi, K. Unexpected Homogeneous Bubble Nucleation Near a Solid-Liquid Interface. *The Journal of Physical Chemistry C*, **122** (50), 28712–28716, 10.1021/acs.jpcc.8b09200 (2018).

16. Shin, D. et al. Growth dynamics and gas transport mechanism of nanobubbles in graphene liquid cells. *Nature Communications*. **6**, 6068, 10.1038/ncomms7068 (2015).

17. Zheng, H., Claridge, S.A., Minor, A.M., Alivisatos, A.P., Dahmen, U. Nanocrystal diffusion in a liquid thin film observed by in situ transmission electron microscopy. *Nano letters*. **9** (6), 2460–2465, 10.1021/nl9012369 (2009).

18. Yuk, J.M. et al. High-resolution EM of colloidal nanocrystal growth using graphene liquid cells. *Science* (New York, N.Y.). **336** (6077), 61–64, 10.1126/science.1217654 (2012).

19. Hauwiller, M.R., Ondry, J.C., Alivisatos, A.P. Using Graphene Liquid Cell Transmission Electron Microscopy to Study in Situ Nanocrystal Etching. *Journal of visualized experiments* (135), 10.3791/57665 (2018).

20. Niu, K.-Y., Liao, H.-G., Zheng, H. Revealing dynamic processes of materials in liquids using liquid cell transmission electron microscopy. *Journal of visualized experiments* (70), 10.3791/50122 (2012).

21. Textor, M., Jonge, N. de Strategies for Preparing Graphene Liquid Cells for Transmission Electron Microscopy. *Nano letters*. **18** (6), 3313–3321, 10.1021/acs.nanolett.8b01366 (2018).

22. Huang, T.-W. et al. Self-aligned wet-cell for hydrated microbiology observation in TEM. *Lab on a chip*. **12** (2), 340–347, 10.1039/c1lc20647h (2012).

23. Dukes, M.J., Moering, J., Damiano, J. Optimization of Liquid Cell Transmission Electron Microscopy for Energy Dispersive X-Ray Spectroscopy. *Microscopy and Microanalysis*. **24** (S1), 304–305, 10.1017/S1431927618002015 (2018).

24. Kelly, D.J. et al. Nanometer Resolution Elemental Mapping in Graphene-Based TEM Liquid Cells. *Nano letters*. **18** (2), 1168–1174, 10.1021/acs.nanolett.7b04713 (2018).

25. Rasool, H., Dunn, G., Fathalizadeh, A., Zettl, A. Graphene-sealed Si/SiN cavities for high-resolution in situ electron microscopy of nano-confined solutions. *Physica Status Solidi (b)*. **253**



(12), 2351–2354, 10.1002/pssb.201600232 (2016).

26. Kröger, R., Verch, A. Liquid Cell Transmission Electron Microscopy and the Impact of Confinement on the Precipitation from Supersaturated Solutions. *Minerals*. **8** (1), 21, 10.3390/min8010021 (2018).

27. Stawski, T.M. et al. “On demand” triggered crystallization of CaCO<sub>3</sub> from solute precursor species stabilized by the water-in-oil microemulsion. *Physical Chemistry Chemical Physics*. **20** (20), 13825–13835, 10.1039/C8CP00540K (2018).

28. Klein, K.L., Anderson, I.M., Jonge, N. de Transmission electron microscopy with a liquid flow cell. *Journal of microscopy*. **242** (2), 117–123, 10.1111/j.1365-2818.2010.03484.x (2011).

29. Hutzler, A., Branscheid, R., Jank, M.P.M., Frey, L., Spiecker, E. Graphene-supported microwell liquid cell for in situ studies in TEM and SEM European Microscopy Congress 2016: Proceedings. Wiley-VCH Verlag GmbH & Co. KGaA. Weinheim, Germany (2016), pp. 209–210.

30. Cho, H. et al. The Use of Graphene and Its Derivatives for Liquid-Phase Transmission Electron Microscopy of Radiation-Sensitive Specimens. *Nano letters*. **17** (1), 414–420, 10.1021/acs.nanolett.6b04383 (2017).

31. Jiang, N. Note on in situ (scanning) transmission electron microscopy study of liquid samples. *Ultramicroscopy*. **179**, 81–83, 10.1016/j.ultramicro.2017.04.012 (2017).

32. Zhu, G., Reiner, H., Cölfen, H., Yoreo, J.J. de Addressing some of the technical challenges associated with liquid phase S/TEM studies of particle nucleation, growth and assembly. *Micron*. **118**, 35–42, 10.1016/j.micron.2018.12.001 (2019).

33. Jonge, N. de, Houben, L., Dunin-Borkowski, R.E., Ross, F.M. Resolution and aberration correction in liquid cell transmission electron microscopy. *Nature Reviews Materials*. **4** (1), 61, 10.1038/s41578-018-0071-2 (2019).

34. Schindelin, J. et al. Fiji: an open-source platform for biological-image analysis. *Nature Methods*. **9** (7), 676, 10.1038/nmeth.2019 (2012).

35. Tinevez, J.-Y. et al. TrackMate: An open and extensible platform for single-particle tracking. *Methods (San Diego, Calif.)*. **115**, 80–90, 10.1016/j.ymeth.2016.09.016 (2017).

36. Oliphant, T.E. Python for Scientific Computing. *Computing in Science & Engineering*. **9** (3), 10–20, 10.1109/MCSE.2007.58 (2007).

37. Millman, K.J., Aivazis, M. Python for Scientists and Engineers. *Computing in Science & Engineering*. **13** (2), 9–12, 10.1109/MCSE.2011.36 (2011).

38. Zaniewski, A.M., Trimble, C.J., Nemanich, R.J. Modifying the chemistry of graphene with substrate selection: A study of gold nanoparticle formation. *Applied Physics Letters*. **106** (12), 123104, 10.1063/1.4916567 (2015).

39. Holtz, M.E., Yu, Y., Gao, J., Abruña, H.D., Muller, D.A. In situ electron energy-loss spectroscopy in liquids. *Microscopy and microanalysis*. **19** (4), 1027–1035, 10.1017/S1431927613001505 (2013).

40. Wang, M., Park, C., Woehl, T.J. Quantifying the Nucleation and Growth Kinetics of Electron Beam Nanochemistry with Liquid Cell Scanning Transmission Electron Microscopy. *Chemistry of Materials*. **30** (21), 7727–7736, 10.1021/acs.chemmater.8b03050 (2018).

41. Woehl, T.J., Abellan, P. Defining the radiation chemistry during liquid cell electron microscopy to enable visualization of nanomaterial growth and degradation dynamics. *Journal of microscopy*. **265** (2), 135–147, 10.1111/jmi.12508 (2017).

42. Ngo, T., Yang, H. Toward Ending the Guessing Game: Study of the Formation of

529 Nanostructures Using In Situ Liquid Transmission Electron Microscopy. *The journal of physical*  
 530 *chemistry letters*. **6** (24), 5051–5061, 10.1021/acs.jpcllett.5b02210 (2015).

531 43. Kraus, T., Jonge, N. de Dendritic gold nanowire growth observed in liquid with transmission  
 532 electron microscopy. *Langmuir*. **29** (26), 8427–8432, 10.1021/la401584z (2013).

533 44. Hauwiller, M.R. et al. Dynamics of Nanoscale Dendrite Formation in Solution Growth  
 534 Revealed Through in Situ Liquid Cell Electron Microscopy. *Nano letters*. **18** (10), 6427–6433,  
 535 10.1021/acs.nanolett.8b02819 (2018).

536 45. Glicksman, M.E. Dendritic Growth. In Nishinga, T., Kuech, T.F., Rudolph, P. (eds.) Handbook  
 537 of crystal growth. Elsevier. Amsterdam (2015), pp. 669–722.

538 46. Li, D. et al. Direction-specific interactions control crystal growth by oriented attachment.  
 539 *Science*. **336** (6084), 1014–1018, 10.1126/science.1219643 (2012).

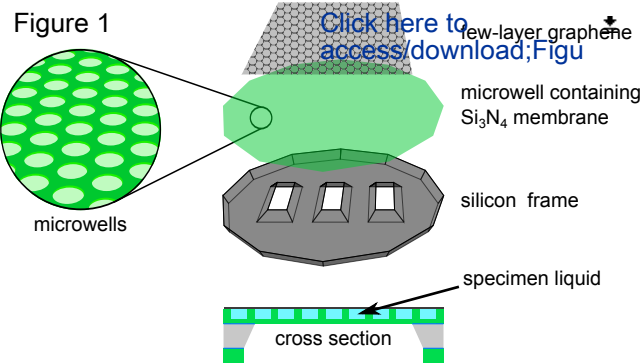
540 47. Dukes, M.J. et al. Improved microchip design and application for in situ transmission electron  
 541 microscopy of macromolecules. *Microscopy and microanalysis*. **20** (2), 338–345,  
 542 10.1017/S1431927613013858 (2014).

543 48. Zaluzec, N.J., Burke, M.G., Haigh, S.J., Kulzick, M.A. X-ray energy-dispersive spectrometry  
 544 during in situ liquid cell studies using an analytical electron microscope. *Microscopy and*  
 545 *Microanalysis*. **20** (2), 323–329, 10.1017/S1431927614000154 (2014).

546 49. Bonn, D., Eggers, J., Indekeu, J., Meunier, J., Rolley, E. Wetting and spreading. *Reviews of*  
 547 *Modern Physics*. **81** (2), 739, 10.1103/RevModPhys.81.739 (2009).

548 50. Karakulina, O.M., Demortière, A., Dachraoui, W., Abakumov, A.M., Hadermann, J. In Situ  
 549 Electron Diffraction Tomography Using a Liquid-Electrochemical Transmission Electron  
 550 Microscopy Cell for Crystal Structure Determination of Cathode Materials for Li-Ion batteries.  
 551 *Nano letters*, 10.1021/acs.nanolett.8b02436 (2018).

Figure 1



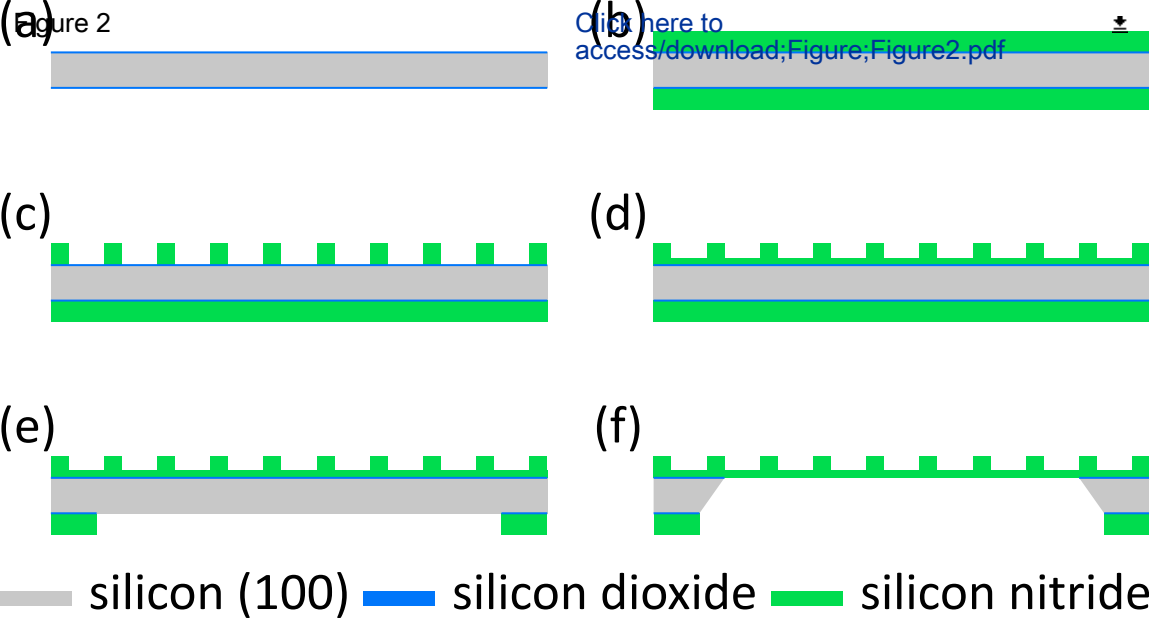
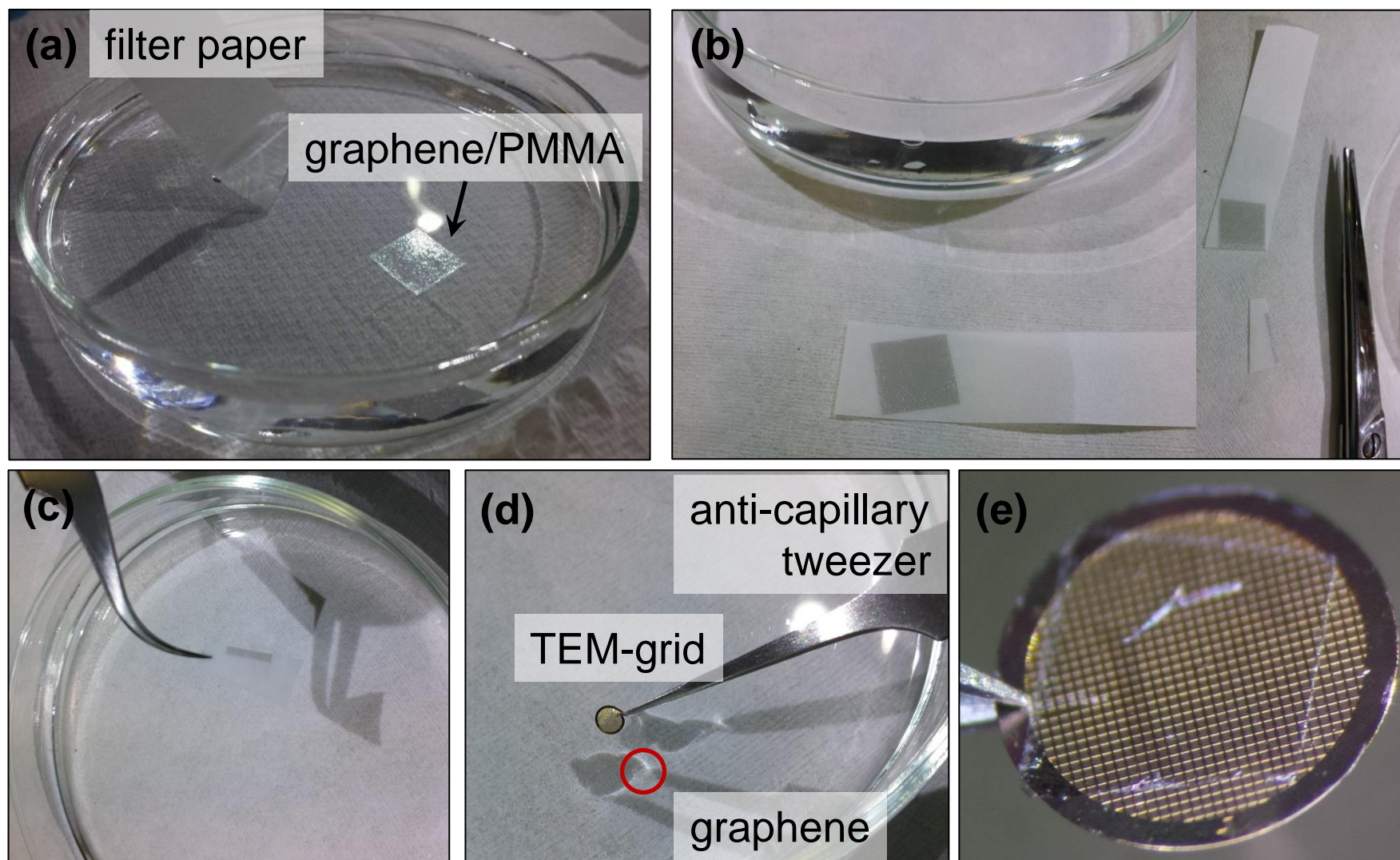
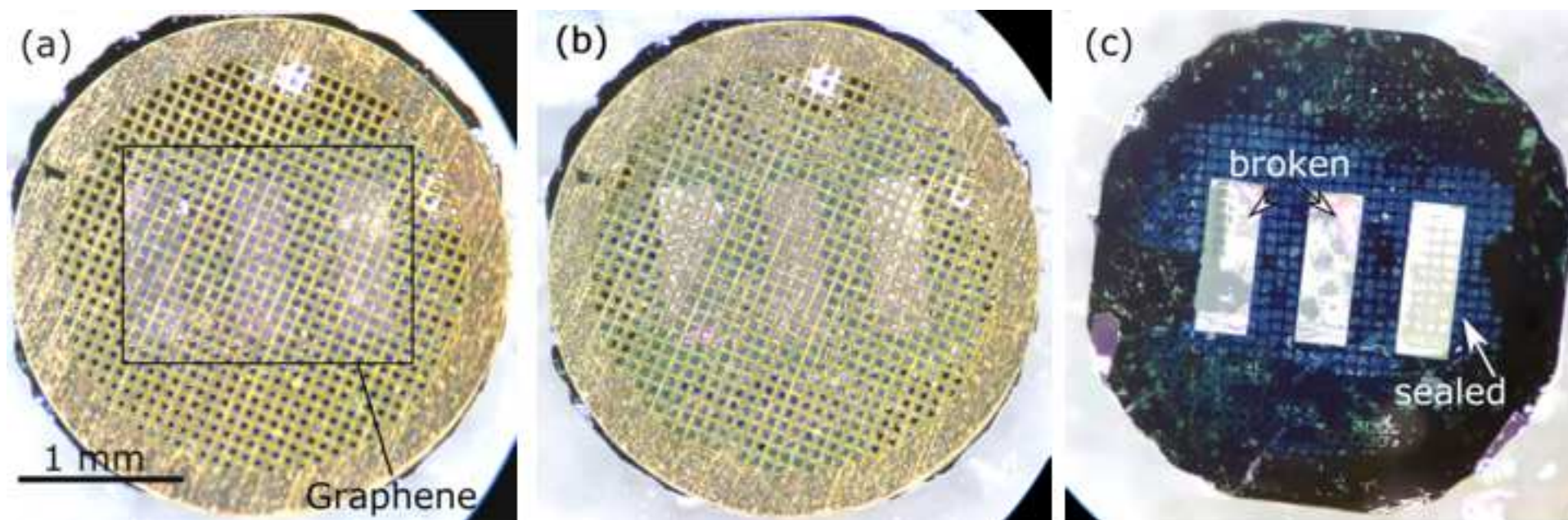
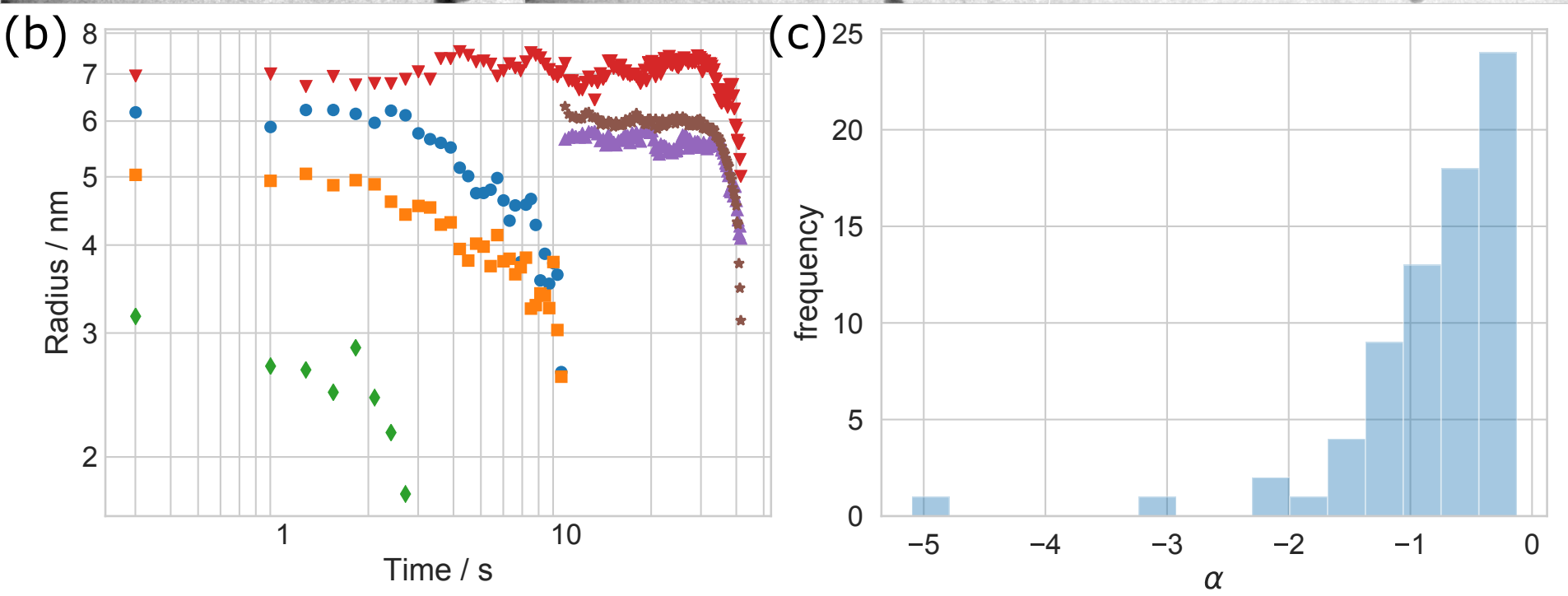
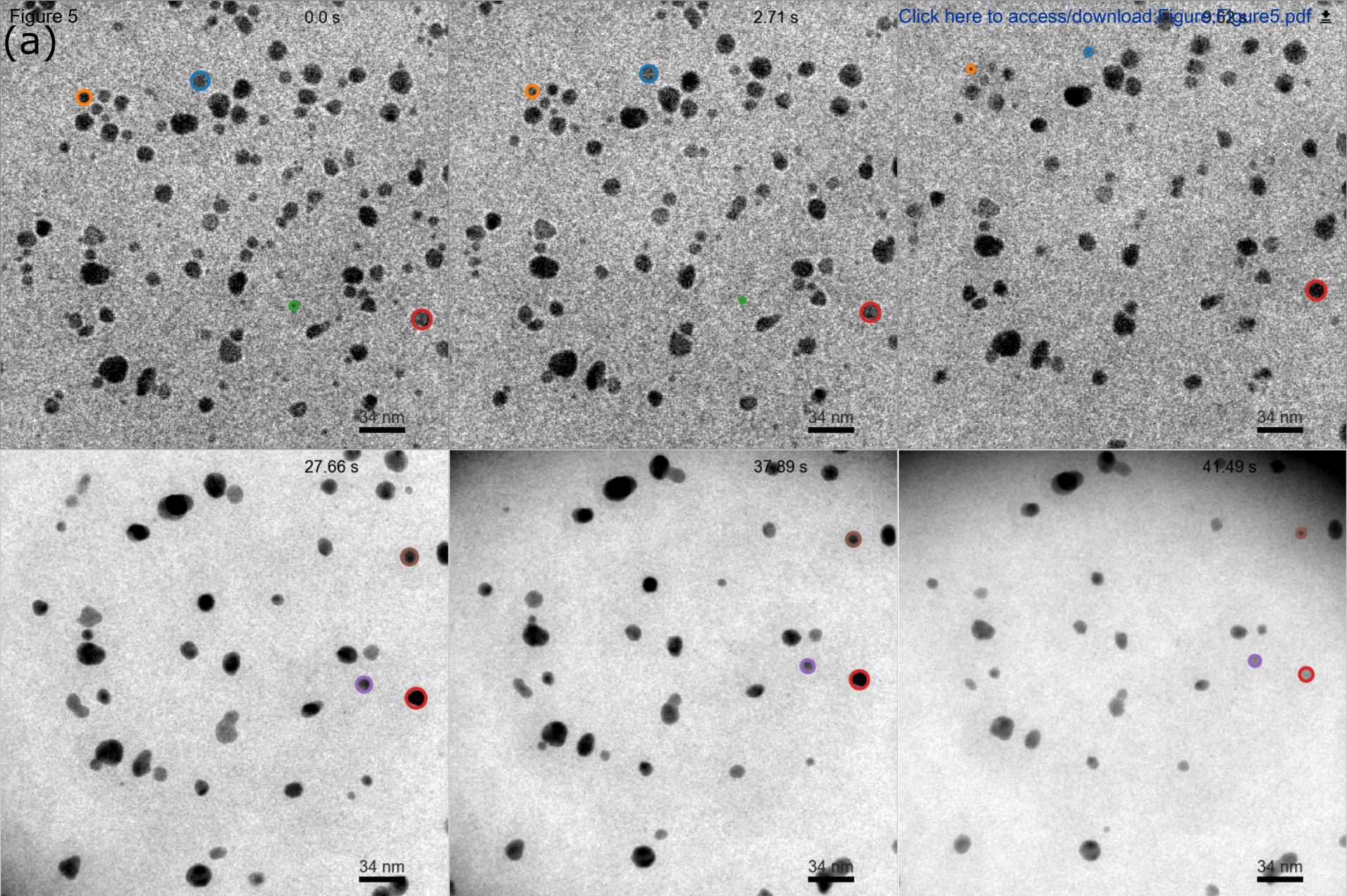


Figure 3











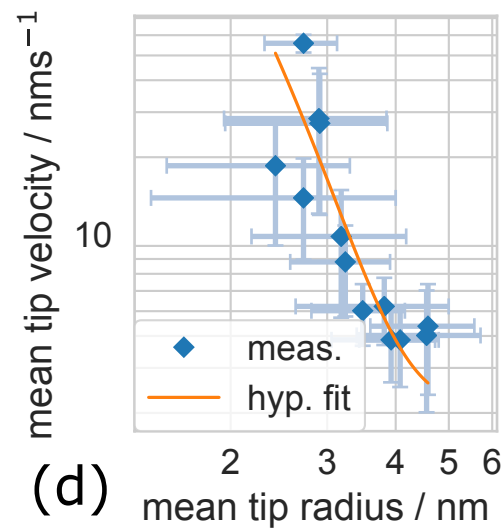
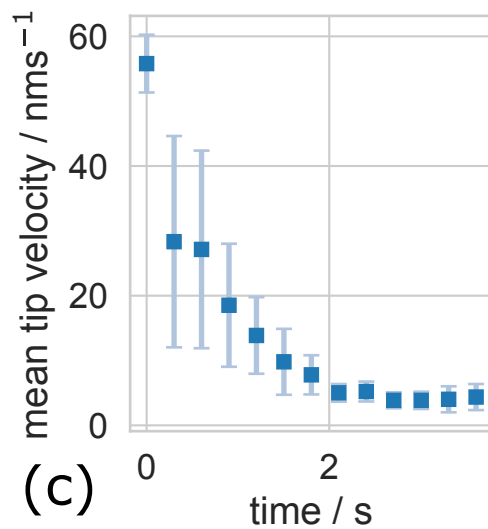
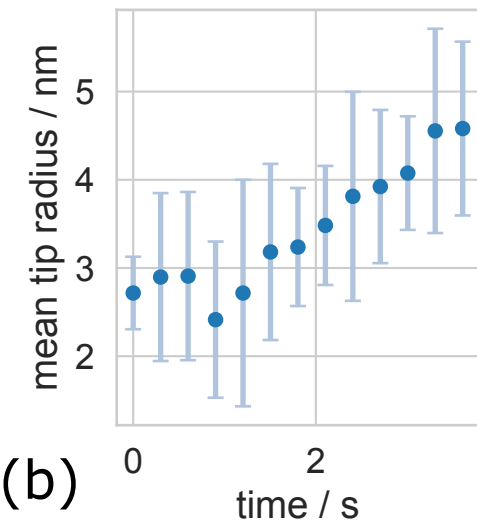
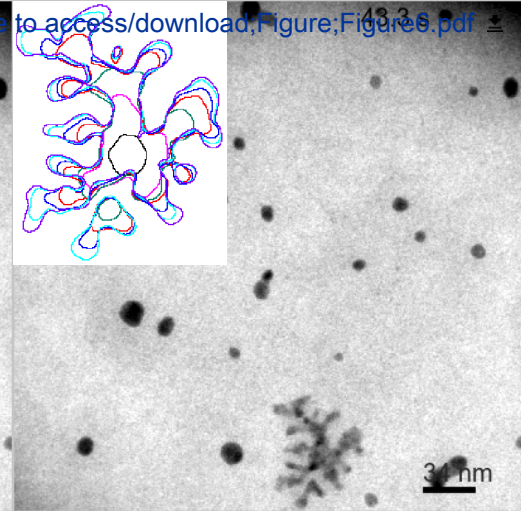
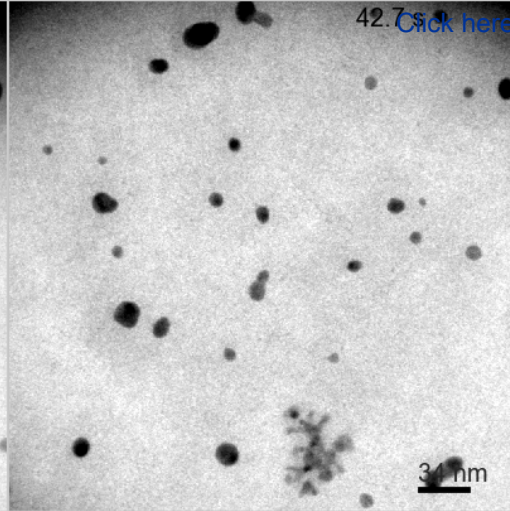
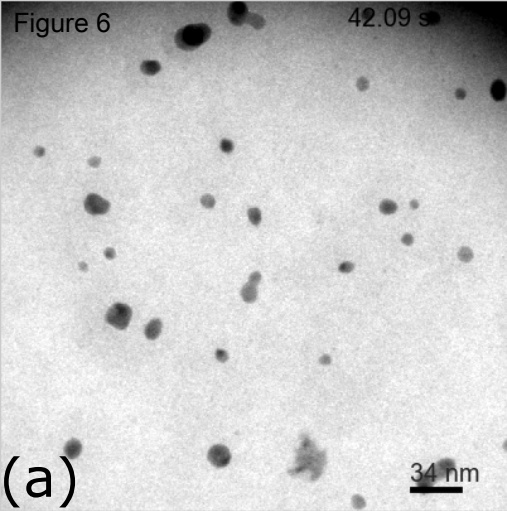
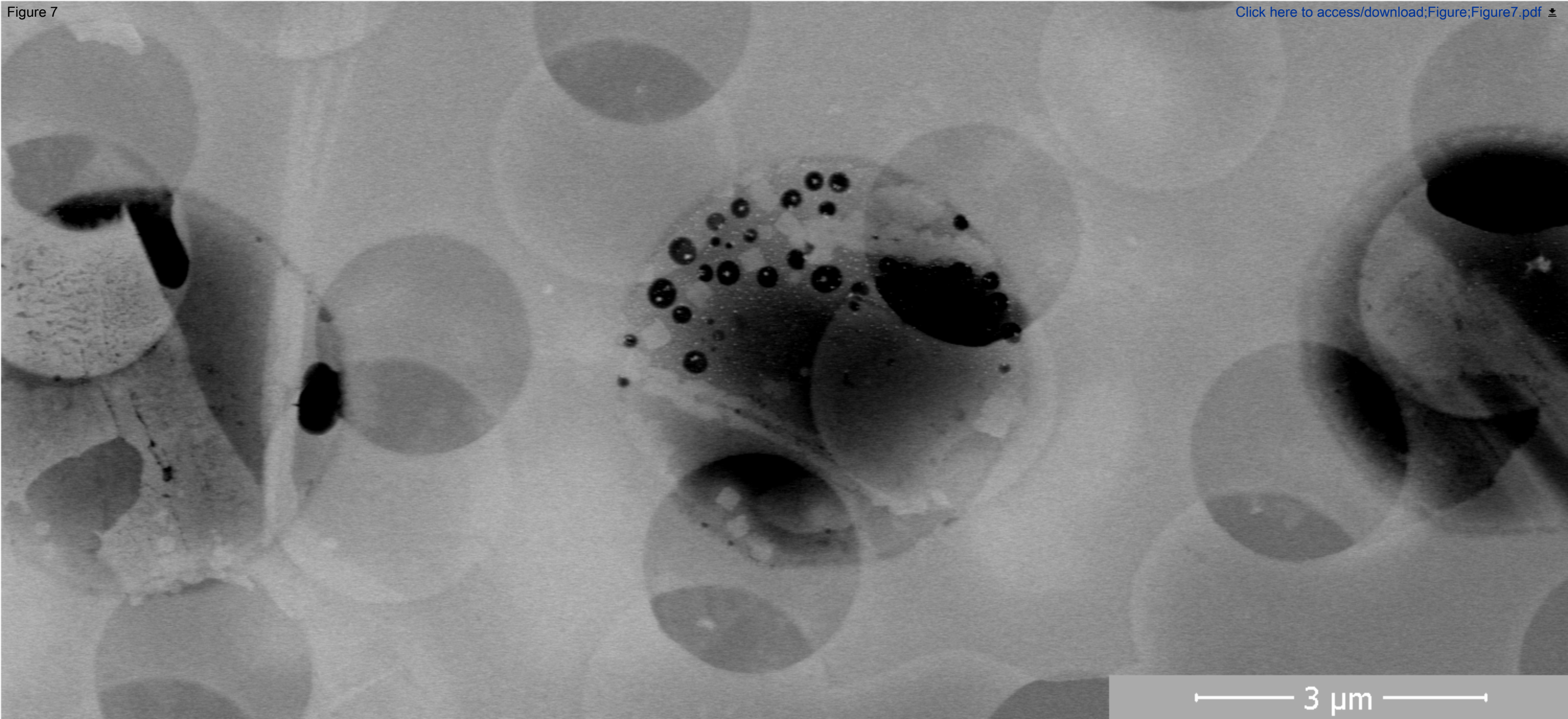




Figure 7

[Click here to access/download;Figure;Figure7.pdf](#)





Click here to access/download  
**Video or Animated Figure**  
Supplementary Video 1.avi



Name of Material/ Equipment	Company	Catalog Number	Comments/Description
Acetone	VWR Chemicals	50488858	VLSI
Deionized water			own production
	Carl Roth GmbH		
Dumont Anti-Capillary tweezers	+ Co. KG	LH72.1	0203-N5AC-PO Dumoxel alloyed
Ethanol	VWR Chemicals	85651.360	VLSI
FIJI Is Just ImageJ	FIJI.sc	Version 1.51	
Gold Quantifoil, Amorphous			
Carbon TEM Grids	Plano GmbH	S173-8	R 2/2 Au 300 mesh
HAuCl <sub>4</sub> · 3 H <sub>2</sub> O crystal	Alfa Aesar	36400.06	5 g
Jupyter Notebook	Project Jupyter	Version 5.7.2	
	John Hunter, Darren Dale, Eric Firing, Michael Droettboom and the Matplotlib development team	Version 3.0.2	
Matplotlib-Package	NumPy		
NumPy-Package	developers	Version 1.15.4	
	AQR Capital Management, LLC, Lambda Foundry, Inc. and PyData Development Team	Version 0.23.4	
Pandas-Package	Python Software Foundation	Version 3.7	
Python	SciPy developers	Version 1.1.0	
Scipy-Package			

Seaborn-Package Michael Waskom Version 0.9.0

Si wafer  
single tilt TEM holder

Siegert Wafer  
GmbH  
Philips

Thin silicon (100) wafer 175 +/-5  $\mu\text{m}$ , 4", p-type, boron doped (1-30 Ohm cm), double-sided polished  
Ensure that cell fits

Transmission Electron Microscope  
Trivial Transfer Graphene

Philips  
ACS Material

CM 30 (S)TEM  
TTG60011

300 kV  
PMMA-covered, 6 -- 8 MLs



## ARTICLE AND VIDEO LICENSE AGREEMENT

Title of Article:

Author(s):

<i>Graphene-supported Microsolv Liquid Cell for In Situ Transmission</i>
<i>Electron Microscopy</i>
<i>A. Huetzel, B. Fritsch, M.P.M. Jauk, R. Branscheid, E. Spiecker, M. März</i>

Item 1: The Author elects to have the Materials be made available (as described at <http://www.jove.com/publish>) via:

☐ Standard Access

☒ Open Access

Item 2: Please select one of the following items:

☒ The Author is **NOT** a United States government employee.

☐ The Author is a United States government employee and the Materials were prepared in the course of his or her duties as a United States government employee.

☐ The Author is a United States government employee but the Materials were NOT prepared in the course of his or her duties as a United States government employee.

### ARTICLE AND VIDEO LICENSE AGREEMENT

1. **Defined Terms.** As used in this Article and Video License Agreement, the following terms shall have the following meanings: “**Agreement**” means this Article and Video License Agreement; “**Article**” means the article specified on the last page of this Agreement, including any associated materials such as texts, figures, tables, artwork, abstracts, or summaries contained therein; “**Author**” means the author who is a signatory to this Agreement; “**Collective Work**” means a work, such as a periodical issue, anthology or encyclopedia, in which the Materials in their entirety in unmodified form, along with a number of other contributions, constituting separate and independent works in themselves, are assembled into a collective whole; “**CRC License**” means the Creative Commons Attribution-Non Commercial-No Derivs 3.0 Unported Agreement, the terms and conditions of which can be found at: <http://creativecommons.org/licenses/by-nc-nd/3.0/legalcode>; “**Derivative Work**” means a work based upon the Materials or upon the Materials and other pre-existing works, such as a translation, musical arrangement, dramatization, fictionalization, motion picture version, sound recording, art reproduction, abridgment, condensation, or any other form in which the Materials may be recast, transformed, or adapted; “**Institution**” means the institution, listed on the last page of this Agreement, by which the Author was employed at the time of the creation of the Materials; “**JoVE**” means MyJoVE Corporation, a Massachusetts corporation and the publisher of The Journal of Visualized Experiments; “**Materials**” means the Article and / or the Video; “**Parties**” means the Author and JoVE; “**Video**” means any video(s) made by the Author, alone or in conjunction with any other parties, or by JoVE or its affiliates or agents, individually or in collaboration with the Author or any other parties, incorporating all or any portion

of the Article, and in which the Author may or may not appear.

2. **Background.** The Author, who is the author of the Article, in order to ensure the dissemination and protection of the Article, desires to have the JoVE publish the Article and create and transmit videos based on the Article. In furtherance of such goals, the Parties desire to memorialize in this Agreement the respective rights of each Party in and to the Article and the Video.

3. **Grant of Rights in Article.** In consideration of JoVE agreeing to publish the Article, the Author hereby grants to JoVE, subject to Sections 4 and 7 below, the exclusive, royalty-free, perpetual (for the full term of copyright in the Article, including any extensions thereto) license (a) to publish, reproduce, distribute, display and store the Article in all forms, formats and media whether now known or hereafter developed (including without limitation in print, digital and electronic form) throughout the world, (b) to translate the Article into other languages, create adaptations, summaries or extracts of the Article or other Derivative Works (including, without limitation, the Video) or Collective Works based on all or any portion of the Article and exercise all of the rights set forth in (a) above in such translations, adaptations, summaries, extracts, Derivative Works or Collective Works and (c) to license others to do any or all of the above. The foregoing rights may be exercised in all media and formats, whether now known or hereafter devised, and include the right to make such modifications as are technically necessary to exercise the rights in other media and formats. If the “Open Access” box has been checked in Item 1 above, JoVE and the Author hereby grant to the public all such rights in the Article as provided in, but subject to all limitations and requirements set forth in, the CRC License.

612542.6 For questions, please contact us at [submissions@jove.com](mailto:submissions@jove.com) or +1.617.945.9051.

## ARTICLE AND VIDEO LICENSE AGREEMENT

4. **Retention of Rights in Article.** Notwithstanding the exclusive license granted to JoVE in **Section 3** above, the Author shall, with respect to the Article, retain the non-exclusive right to use all or part of the Article for the non-commercial purpose of giving lectures, presentations or teaching classes, and to post a copy of the Article on the Institution's website or the Author's personal website, in each case provided that a link to the Article on the JoVE website is provided and notice of JoVE's copyright in the Article is included. All non-copyright intellectual property rights in and to the Article, such as patent rights, shall remain with the Author.

5. **Grant of Rights in Video – Standard Access.** This **Section 5** applies if the "Standard Access" box has been checked in **Item 1** above or if no box has been checked in **Item 1** above. In consideration of JoVE agreeing to produce, display or otherwise assist with the Video, the Author hereby acknowledges and agrees that, Subject to **Section 7** below, JoVE is and shall be the sole and exclusive owner of all rights of any nature, including, without limitation, all copyrights, in and to the Video. To the extent that, by law, the Author is deemed, now or at any time in the future, to have any rights of any nature in or to the Video, the Author hereby disclaims all such rights and transfers all such rights to JoVE.

6. **Grant of Rights in Video – Open Access.** This **Section 6** applies only if the "Open Access" box has been checked in **Item 1** above. In consideration of JoVE agreeing to produce, display or otherwise assist with the Video, the Author hereby grants to JoVE, subject to **Section 7** below, the exclusive, royalty-free, perpetual (for the full term of copyright in the Article, including any extensions thereto) license (a) to publish, reproduce, distribute, display and store the Video in all forms, formats and media whether now known or hereafter developed (including without limitation in print, digital and electronic form) throughout the world, (b) to translate the Video into other languages, create adaptations, summaries or extracts of the Video or other Derivative Works or Collective Works based on all or any portion of the Video and exercise all of the rights set forth in (a) above in such translations, adaptations, summaries, extracts, Derivative Works or Collective Works and (c) to license others to do any or all of the above. The foregoing rights may be exercised in all media and formats, whether now known or hereafter devised, and include the right to make such modifications as are technically necessary to exercise the rights in other media and formats. For any Video to which this **Section 6** is applicable, JoVE and the Author hereby grant to the public all such rights in the Video as provided in, but subject to all limitations and requirements set forth in, the CRC License.

7. **Government Employees.** If the Author is a United States government employee and the Article was prepared in the course of his or her duties as a United States government employee, as indicated in **Item 2** above, and any of the licenses or grants granted by the Author hereunder exceed the scope of the 17 U.S.C. 403, then the rights granted hereunder shall be limited to the maximum

rights permitted under such statute. In such case, all provisions contained herein that are not in conflict with such statute shall remain in full force and effect, and all provisions contained herein that do so conflict shall be deemed to be amended so as to provide to JoVE the maximum rights permissible within such statute.

8. **Protection of the Work.** The Author(s) authorize JoVE to take steps in the Author(s) name and on their behalf if JoVE believes some third party could be infringing or might infringe the copyright of either the Author's Article and/or Video.

9. **Likeness, Privacy, Personality.** The Author hereby grants JoVE the right to use the Author's name, voice, likeness, picture, photograph, image, biography and performance in any way, commercial or otherwise, in connection with the Materials and the sale, promotion and distribution thereof. The Author hereby waives any and all rights he or she may have, relating to his or her appearance in the Video or otherwise relating to the Materials, under all applicable privacy, likeness, personality or similar laws.

10. **Author Warranties.** The Author represents and warrants that the Article is original, that it has not been published, that the copyright interest is owned by the Author (or, if more than one author is listed at the beginning of this Agreement, by such authors collectively) and has not been assigned, licensed, or otherwise transferred to any other party. The Author represents and warrants that the author(s) listed at the top of this Agreement are the only authors of the Materials. If more than one author is listed at the top of this Agreement and if any such author has not entered into a separate Article and Video License Agreement with JoVE relating to the Materials, the Author represents and warrants that the Author has been authorized by each of the other such authors to execute this Agreement on his or her behalf and to bind him or her with respect to the terms of this Agreement as if each of them had been a party hereto as an Author. The Author warrants that the use, reproduction, distribution, public or private performance or display, and/or modification of all or any portion of the Materials does not and will not violate, infringe and/or misappropriate the patent, trademark, intellectual property or other rights of any third party. The Author represents and warrants that it has and will continue to comply with all government, institutional and other regulations, including, without limitation all institutional, laboratory, hospital, ethical, human and animal treatment, privacy, and all other rules, regulations, laws, procedures or guidelines, applicable to the Materials, and that all research involving human and animal subjects has been approved by the Author's relevant institutional review board.

11. **JoVE Discretion.** If the Author requests the assistance of JoVE in producing the Video in the Author's facility, the Author shall ensure that the presence of JoVE employees, agents or independent contractors is in accordance with the relevant regulations of the Author's institution. If more than one author is listed at the beginning of this Agreement, JoVE may, in its sole



## ARTICLE AND VIDEO LICENSE AGREEMENT

discretion, elect not take any action with respect to the Article until such time as it has received complete, executed Article and Video License Agreements from each such author. JoVE reserves the right, in its absolute and sole discretion and without giving any reason therefore, to accept or decline any work submitted to JoVE. JoVE and its employees, agents and independent contractors shall have full, unfettered access to the facilities of the Author or of the Author's institution as necessary to make the Video, whether actually published or not. JoVE has sole discretion as to the method of making and publishing the Materials, including, without limitation, to all decisions regarding editing, lighting, filming, timing of publication, if any, length, quality, content and the like.

12. **Indemnification.** The Author agrees to indemnify JoVE and/or its successors and assigns from and against any and all claims, costs, and expenses, including attorney's fees, arising out of any breach of any warranty or other representations contained herein. The Author further agrees to indemnify and hold harmless JoVE from and against any and all claims, costs, and expenses, including attorney's fees, resulting from the breach by the Author of any representation or warranty contained herein or from allegations or instances of violation of intellectual property rights, damage to the Author's or the Author's institution's facilities, fraud, libel, defamation, research, equipment, experiments, property damage, personal injury, violations of institutional, laboratory, hospital, ethical, human and animal treatment, privacy or other rules, regulations, laws, procedures or guidelines, liabilities and other losses or damages related in any way to the submission of work to JoVE, making of videos by JoVE, or publication in JoVE or elsewhere by JoVE. The Author shall be responsible for, and shall hold JoVE harmless from, damages caused by lack of sterilization, lack of cleanliness or by contamination due to

the making of a video by JoVE its employees, agents or independent contractors. All sterilization, cleanliness or decontamination procedures shall be solely the responsibility of the Author and shall be undertaken at the Author's expense. All indemnifications provided herein shall include JoVE's attorney's fees and costs related to said losses or damages. Such indemnification and holding harmless shall include such losses or damages incurred by, or in connection with, acts or omissions of JoVE, its employees, agents or independent contractors.

13. **Fees.** To cover the cost incurred for publication, JoVE must receive payment before production and publication the Materials. Payment is due in 21 days of invoice. Should the Materials not be published due to an editorial or production decision, these funds will be returned to the Author. Withdrawal by the Author of any submitted Materials after final peer review approval will result in a US\$1,200 fee to cover pre-production expenses incurred by JoVE. If payment is not received by the completion of filming, production and publication of the Materials will be suspended until payment is received.

14. **Transfer, Governing Law.** This Agreement may be assigned by JoVE and shall inure to the benefits of any of JoVE's successors and assignees. This Agreement shall be governed and construed by the internal laws of the Commonwealth of Massachusetts without giving effect to any conflict of law provision thereunder. This Agreement may be executed in counterparts, each of which shall be deemed an original, but all of which together shall be deemed to me one and the same agreement. A signed copy of this Agreement delivered by facsimile, e-mail or other means of electronic transmission shall be deemed to have the same legal effect as delivery of an original signed copy of this Agreement.

A signed copy of this document must be sent with all new submissions. Only one Agreement is required per submission.

### CORRESPONDING AUTHOR

Name:

<i>Andreas Hutzler</i>
<i>Electron Devices, Department of Electrical, Electronic and Communication Engineering</i>
<i>Friedrich-Alexander University Erlangen-Nürnberg</i>
<i>Dr.-Ing.</i>

Department:

Institution:

Title:

Signature:

<i>A. Hutzler</i>	Date: <i>30.01.2019</i>
-------------------	-------------------------

Please submit a **signed** and **dated** copy of this license by one of the following three methods:

1. Upload an electronic version on the JoVE submission site
2. Fax the document to +1.866.381.2236
3. Mail the document to JoVE / Attn: JoVE Editorial / 1 Alewife Center #200 / Cambridge, MA 02140

612542.6 For questions, please contact us at submissions@jove.com or +1.617.945.9051.

Dear editor,

At first we like to thank you for critically reviewing our manuscript which helped to further improve its quality. All suggested comments were carefully addressed and implemented as discussed in a point-by-point answer below.

The editorial comments as well as the comments of the two referees are inserted as black text and our point-by-point answer is written in blue for easier differentiation. Additionally, phrases which explicitly address distinct comments are marked **bold** and text passages directly reprinted from the manuscript are formatted *italic*. If literature is mentioned that is not referenced in the manuscript, the respective DOI is added.

### Editorial comments:

1. Please take this opportunity to thoroughly proofread the manuscript to ensure that there are no spelling or grammar issues.

A careful proofreading has been performed and some minor changes were done in the manuscript.

2. Please obtain explicit copyright permission to reuse any figures from a previous publication. Explicit permission can be expressed in the form of a letter from the editor or a link to the editorial policy that allows re-prints. Please upload this information as a .doc or .docx file to your Editorial Manager account. The Figure must be cited appropriately in the Figure Legend, i.e. “This figure has been modified from [citation].”

Permission for reuse of figure **Figure 1** was **granted** and an **appropriate citation** as well as **information about the copyright** is given in the **figure caption**. Additionally, the **information** about the granted permission is **uploaded into the Editorial Manager account**.

3. Please sort the items in alphabetical order according to the name of material/equipment.

As suggested, the **material list** has been **sorted in alphabetical** order.

4. Please add a one-line space between each of your protocol steps.

We have followed your suggestion and reformatted the protocol section accordingly by inserting a **one-line space between each protocol step**.

5. Step 3.1: How to prepare the specimen? Please add more details.

We have created a stock solution by following standard chemistry procedures to create a solution with a defined precursor concentration. The respective amount of water and crystals are added in the **protocol step 3.1** in the following way:

*3.1. Prepare the specimen for incorporation in the GSMLC. To do so, prepare a 1 mM stock solution by solving 196.915 mg  $\text{HAuCl}_4 \cdot 3 \text{H}_2\text{O}$  crystals in 0.5 l deionized water. To do*



*so, prepare a 1 mM stock solution by solving 196.915 mg of  $\text{HAuCl}_4 \cdot 3 \text{H}_2\text{O}$  crystals in 0.5 l deionized water.*

#### 6. 4.2: How to apply the plasma?

The details for the plasma treatment were added to the protocol:

*4.2 Apply an **ambient  $\text{O}_2/\text{N}_2$  (20% / 80%) plasma** for 5 min to enhance the wettability of the membrane.*

#### 7. 4.4: Please split this step into more sub-steps so that each step contains only 2-3 actions.

We have followed your suggestion and split the paragraph accordingly into two steps with two (4.4) and one (4.5) actions as follows:

***4.4 Place the TEM grid** onto the micro-patterned  $\text{Si}_3\text{N}_4$  layer with the graphene facing the template. **Press the graphene-coated TEM grid onto the template.** Be careful not to destroy the bottom  $\text{Si}_3\text{N}_4$  membrane.*

***4.5 Remove excess solution** with a tissue to accelerate the cell drying and thus mitigate concentration changes (Figure 4(a)). After approx. 2 – 3 min, the graphene- $\text{Si}_3\text{N}_4$  van-der-Waals interaction sufficiently seals the liquid cell (Figure 4(b)). Alternatively, the cell can be left to dry out completely without removing the excess solution. The latter offers a higher success rate in the cell processing. However, evaporation-based concentration changes in the specimen solution are expected to be more severe when using this approach.*

## Reviewers' comments:

### Reviewer #1:

#### Manuscript Summary:

The authors present the method for a hybrid graphene-silicon nitride liquid cell for electron microscopy imaging. Liquid cell electron microscopy is a popular field, so this interesting technique could potentially be used by other groups. They have demonstrated this technique using the growth of gold nanoparticles and shown how the resulting videos can be analyzed. The authors make some bold claims about how their technique relates to others in the field and adding data to back up those claims would be useful. Otherwise, a smattering of minor improvements, including details in the protocol, would improve the manuscript to a publishable level.

#### Major Concerns:

1. The authors state one of the main advantages of this method is the reduction in window bulging (Abstract, Discussion) and "reproducibly shaped cells with tailored liquid thickness" (line 86-87 in Introduction). Do the authors have any measurements that show the reproducible liquid thickness and lack of bulging?

Thank you for your question. As a similar question was also asked by the second reviewer, we included a SEM image (Figure 7 in the manuscript) showing that we have a wrinkled graphene membrane, but **no bulging-related layer thickness increase**. Close to the well edge, the **liquid thickness equals the well height**. In SiLCs, a similar approach is performed to bypass the severe membrane bulging caused by large membranes, whereas in GLCs no liquid thickness control can be performed. Albeit we cannot ensure a homogeneous layer thickness over the whole cell, **our approach allows similar thickness tailoring as in SiLCs**. Furthermore, by choosing a microwell design **we reduce the maximum membrane bulging** because the membrane area itself is reduced significantly, which has been demonstrated by Dukes et al. (2014) for microwell-based SiLCs. We understand your concern and therefore **adjusted our discussion section**:

*Moreover, **large viewing areas** can be realized without severe window bulging due to the small membrane areas of the individual specimen chambers. Thereby, **bulging-related thickness increase**<sup>33</sup> can be ruled out to a large extent as shown by Dukes et al.<sup>47</sup>.*

2. The authors claim that this technique "outperforms both, Si technology-based, and graphene liquid cell setups, by combining their most striking aspects" (line 280-281) While the authors show that it combines aspects of both techniques, there is not much data showing that their technique is superior to the existing techniques. For example, the authors say their technique is "utilizing the shielding effects of graphene layers" (line 87-88) Can they show that having only one side of graphene maintains these advantages? If a particle is on the silicon nitride window, does it still feel the effect of the graphene?

Thank you again for your highly valued remark on this issue. We hope that the following explanation might dispel your concerns:

Shielding effects by the graphene are twofold: First, its conductivity might reduce membrane charging. As the **electron beam passes the graphene membrane first**, where the charging effects are believed to be more severe due to the lack of beam scattering, we believe that this

**shielding effect will also be present in GSMLCs.** However, due to the insulating silicon nitride membrane, **there still might be a charging effect in the cell.** Second, Cho et al. (2017) showed that **graphene scavenges radicals.** Due to the **small liquid thickness** of maximal 190 nm in the present case, **this effect should reduce radical concentrations in the whole cell.** Still, we are aware of the fact that in the study presented here, we utilize these species to provoke etching (as has been done in GLCs, as well). For clarity, we adjusted the respective paragraph to the following format:

*Their Si technology-based frame allows for mass production of reproducibly shaped cells with tailored liquid thickness and extra-thin membranes from a single wafer. The graphene membrane covering these cells **also mitigates electron beam-induced perturbations**<sup>8,30,31</sup> since the **electron beam passes through the top graphene membrane first.***

Potentially a better way to phrase line 280-281 would be "The GSMLC architecture demonstrated here combines aspects of Silicon Nitride and graphene liquid cells that could potentially lead to unique advantages."

Thank you for your suggestion for a reformulation. We agree with your concern and decided to **include your wording** in the respective paragraph.

3. In JoVE articles, it is helpful for authors to explain the failure modes to the readers- what are the most common ways for "messaging up" and how can the reader avoid those mistakes. The authors mention that dedicated training is required, but a more specific exploration of common mistakes would be very useful.

Thank you very much for your insight into this issue. We would like to illuminate the answer to your remark in the following:

The most prominent way to "mess up" the preparation of a GSMLC lies within the **graphene transfer and the subsequent TEM grid removal.** Based on your comment, we **adjusted the wording** by adding notes to protocol steps 2.4 and 2.6 as follows:

2.4 [...] *NOTE: Take care that the **graphene site of the graphene-PMMA stack stays on top during the whole procedure.** Otherwise, the subsequent PMMA-removal will lift-off the graphene layer.*

2.6 [...] *NOTE: Use **a flat vessel** (e.g. a petri dish) to simplify the specimen transfer afterwards.*

Furthermore, we elucidated the TEM grid lift-off in protocol 4.6:

4.6 *Carefully remove the TEM grid with a tweezer by pushing a tweezer tip between the grid and the GSMLC frame.*

*NOTE: **Rash movements might break the underlying membrane.** To reduce shear force damage, start from the grid site parallel to the smaller window edge.*

Additionally, the importance of that step is **emphasized in the discussion** section:

*Here, the **most sensitive preparation step is the TEM-grid removal after the graphene transfer, because rash movements or jittering is likely to break the Si<sub>3</sub>N<sub>4</sub> layer.** The*

*redundant membrane windows, however, enhance the chances of preserving at least one membrane area.*

#### Minor Concerns:

4. Silicon Nitride should probably appear in the title. For example, "Hybrid Graphene-Silicon Nitride Microwell Liquid Cell for In Situ Transmission Electron Microscopy"

Thank you for your title suggestion. We agree that mentioning Silicon Nitride in the title might be a feasible option. However, in order to be consistent with our previous work published on this cell architecture, we decided to keep the name of the cell. Also, **the phrase ‘microwell’ is used by other groups for Silicon Nitride-based systems** (for example Dukes 2014, Noh 2018 (DOI: 10.1017/S1431927618001988)). By adapting to it and including it in the name of our architecture we still hope to follow the spirit of your concern.

Nevertheless, if you or the editor strongly disagrees with this argumentation, we would of course change it.

5. Are these liquid cells full of liquid, or are they thin layers of liquid on the top and bottom windows? Both methods are common in the literature. Evidence confirming which regime this technique operates in would be helpful.

A representative **HAADF SEM image of a loaded GSMLC in STEM mode** at low acceleration voltage (29 kV) is now displayed as **Figure 7**. It is clearly visible that the membrane shading stays mostly constant over the well region, but darkens towards the well center. This accounts for **negative bulging** and is illustrated in the Figure below, where intensity cross sections of the wells visible in **Figure 7** are displayed (see **Figure A**).

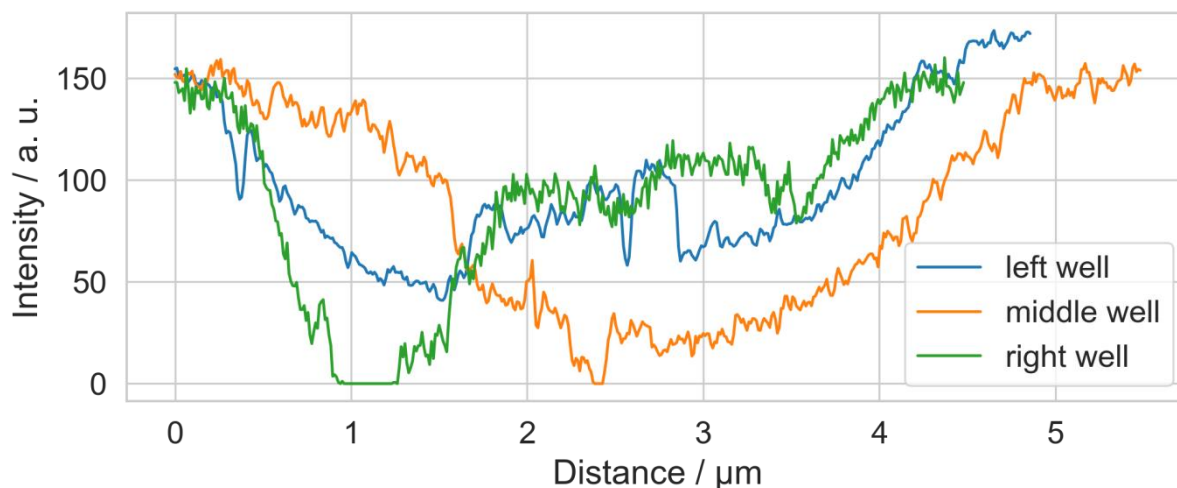


**Figure A:** Intensity cross section of the wells displayed in Figure 7 of the manuscript.

This phenomenon is discussed with respect to analyses performed by Kelly et al.. They demonstrated that the negative bulging and (partial) well drying visible in **Figure 7** is directly **depending on the well diameter. Reducing the latter is therefore a feasible approach to homogenize the liquid thickness even further.**

The **liquid thickness is expected to be below 190 nm.** The shown SEM micrograph supports this assumption. However, we observe **gas bubble formation** at the end of the provided

supplementary video. Without liquid, this would be impossible. Also, dynamic processes such as the apparent **gold ion transport** to the supersaturated area of the dendrite growth are observed. This **contradicts with a negligible liquid thickness**. Based on these assumptions we expect a **liquid thickness between 50 and 100 nm**. However, as the utilized TEM does not support EELS or STEM-based liquid thickness measurements, we cannot provide a measurement for this dedicated experiment. We have **adjusted the discussion section** by incorporating Figure 7 and the following paragraph:

*Thereby, bulging-related thickness increase<sup>33</sup> can be ruled out to a large extent, as shown by Dukes et al.<sup>47</sup>. This is demonstrated in Figure 7, where a representative high-angle annular dark field (HAADF) STEM image of a loaded GSMLC is displayed. This image was acquired using a FEI Helios NanoLab 660 SEM/FIB Dual-beam system. Since the image brightness acquired in this setup is directly related to the specimen thickness, it is clearly visible that the sealed microwells exhibit only small negative bulging. Kelly et al.<sup>24</sup> have demonstrated that the negative bulging and partial well drying visible in Figure 7 depends on the well diameter. Reducing the well diameter is therefore a feasible approach to homogenize the liquid thickness even further.*

6. In line 265, the authors say that  $\alpha$  is based on 73 "sufficiently monitored" dissolving particles. What does "sufficiently monitored" mean?

All 73 particles are cross-validated using the complementary detection methods of *Analyze Particles* and *TrackMate* of FIJI to rule out false positives. Furthermore, only particles where the radius decline can be explained using an allometric model with an adjusted coefficient of determination of at least 75% are regarded. We adjusted the manuscript to clarify this issue:

*Figure 5 (c) shows the distribution of  $\alpha$  based on 73 dissolving particles from the present study. Only particles where an allometric model explains the decline to at least 75% (adjusted coefficient of determination) are regarded.*

7. Dendrites form in a supersaturated solution. How can dendrites form while nearby particles also etch? Are they on opposite windows? Is the composition different on each window?

Thank you for your question. We included the following paragraph into the manuscript to clarify this issue for the reader:

*Dendrite growth is caused by **local supersaturation** of Au-ions due to the aforementioned particle etching. In Figure 5(a), it is clearly visible that particles are still dissolving whilst the oversaturated system relaxes into dendrite growth. This may be caused by local concentration variations in both, the Au-ions and the oxidative species that could **result from a high viscosity** of the liquid in the GSMLC which has been observed before<sup>6</sup>. A detailed discussion of this phenomenon, however, is beyond the scope of this work.*

An option would be to reference to the PhD thesis of the author, where a detailed discussion of the phenomenon is shown.

8. How is the dendrite tip radius and velocity measured? Is it measured with the same software as described in the manuscript? Outlines on the figures could be helpful.

The outlines were extracted and analyzed using **FIJI**. In order to help the reader to follow our analysis, the dendrite outline development is now included into **Figure 6** in the manuscript. Furthermore, an additional step was added to the protocol:

*5.3.5. Use FIJI to extract the precise contours of more complex structures such as dendrites. Here, Analyze Particles can be applied, as well (see inset of Figure 6 (a)).*

*NOTE: It might be feasible to analyze features of interest manually.*

9. Plotting mean tip velocity vs. mean tip radius on a log-log plot may make it easier to compare with classical models

We adjusted **Figure 6d** by **plotting** the tip radius against the tip velocity in a **logarithmic scale** in accordance to your suggestion.

10. The authors discuss how fabricating the Silicon Nitride layer allows smaller membranes enabling HRTEM. Citing Haimei Zheng's and others work using homemade silicon nitride liquid cells to achieve atomic resolution would be good.

We thank the reviewer for this advice and adjusted the wording in the manuscript, so that it becomes clear that HRTEM is also possible with SiLCs and has been shown by the group of Haimei Zheng and others.

11. Additionally, they suggest they can do HRTEM of gold nanocrystals in their liquid cell. Including an example image would be nice.

Unfortunately, **in the experiment demonstrated here, we did not yield atomic resolution. Adding images** from a different experiment **might confuse the reader** as this information would not be included in the supplementary video. To prove our statement, we adjusted the manuscript and **referenced previously published work** of our group, which is available under an open access license. If wished by the editor, we can also provide a supplementary figure from a comparable experiment showing HRTEM.

12. Does this method work for solvents beyond water similar to silicon nitride and graphene liquid cells?

Thank you for this intriguing question. Until today, we have only performed experiments based on aqueous solutions. However, as the sealing is based on van der Waals interactions, the respective **surface energy of the specimen and its Hamaker constant** are determining whether an encapsulation is possible. As we have performed **high quality work with solutions containing CTAB** (Hutzler et al. 2018), **which is amphiphilic** and thus creates **complementary interface conditions** to pure water, we have broad hint that our approach is **applicable to a vast range of specimen solutions**, similar to SiLCs and GLCs.

13. The authors state that their yield of GSMLCs is above 75%, but in the example they show only one of the 3 wells successfully contains liquid. Is this just a poor example, or is the greater than 75% yield estimate a little too optimistic?



We understand the concern about the stated value. As JoVE requires a positive and a negative working example, we tried to kill two birds with one stone by showing an intermediate result which can be used to explain both scenarios on one image. Also, **it is crucial to distinguish between the cell itself** (TEM grid-sized frame including window areas with microwells), **window areas** (three macroscopic rectangles containing a microwell pattern) **and the circular microwells** themselves. To clarify this architecture, **we added a schematic of the cell architecture** as **Figure 1**. Consequently, by using the term ‘yield’ we do not address the amount of intact window areas, but the **ratio of cells that can be utilized** after performing the loading procedure described here. By showing this particular working example with only one remaining window area, we hope to **underline the advantage of introducing several window areas**, as this redundancy yields in a higher chance of maintaining at least one area during the preparation. We have adjusted the manuscript accordingly in the following way:

*The redundant membrane windows, however, enhance the chances to preserve at least one membrane area. As a consequence, the yield (amount operable GSMLC chips) achieved by a trained experimenter is three out of four<sup>6</sup>, and thus exceeds the one achieved with graphene-based cells (one to two out of four)<sup>19</sup>.*

14. The authors use of "exemplary" seems odd. I think they mean representative.

Thank you for this remark; we have replaced the phrase *exemplary* by *representative*, as suggested.

## 15. Protocol details

\* In Step 2.1, it would be helpful to state the number of monolayers of graphene. (I know it is in the materials section, but I think it is useful to include here, too.)

As suggested, the number of graphene layers (**6-8**) was additionally mentioned under step 2.1 in the protocol.

\* In Step 2.6, how does the rinse occur? How much liquid? Is it dipped in or sprayed?

An additional statement concerning the rinsing was added in the manuscript:

*Remove the PMMA protection layer in an acetone bath for 30 min and consecutively add further cleaning steps by **immersing** in ethanol and DI water without drying the sample in between.*

**NOTE: Use a flat vessel (e.g. a petri dish) to simplify the specimen transfer afterwards.**

\* In Step 2.7, how long should the sample dry for?

The drying time (**30 min**) was additionally mentioned in the manuscript.

\* In Step 3.1, the units of 1 mM/l seem odd.

Thank you for this hint. The unit was changed to **1 mM**.

\* In Step 4.2, how long is the O<sub>2</sub>/N<sub>2</sub> plasma and at what conditions?

Time and plasma conditions were added to the manuscript:

*Apply an ambient O<sub>2</sub>/N<sub>2</sub> (20% / 80%) plasma for **5 min** to enhance the wettability of the membrane.*

\* In Step 4.3, what volume of liquid is deposited onto the template?

The liquid volume (**0.1 µl**) which is deposited onto the template was additionally mentioned in the manuscript:

*3.2 Take the desired amount of specimen from the stock solution. Here, **0.1 µl** is applied. This can be done by using a syringe or an Eppendorf pipette.*

\* Does the liquid dry out at all while the pocket is being made? The authors state that they can "achieve a precise analyte concentration in the cell" (Line 151-152) Do they have any evidence that the liquid is the same concentration?

Unfortunately, we do not have such evidence. To adjust to your valuable remark, we mitigated the mentioned phrase as stated below:

*Remove excess solution with a tissue to fasten the cell drying and thus mitigate concentration changes (Figure 4(a)). After approx. 2 – 3 min, the graphene-Si<sub>3</sub>N<sub>4</sub> van-der-Waals interaction sufficiently seals the liquid cell (Figure 4(b)). Alternatively, the cell can be left to dry out completely without removing the excess solution. The latter offers a higher success rate in the cell processing. However, evaporation-based concentration changes in the specimen solution are expected to be more severe when using this approach.*

The removal of excess solution minimizes the concentration change caused by evaporation because less liquid has to evaporate before the cell is sealed. The problem addressed here, however, might also adjust to standard liquid cells, as a precise concentration measurement of specimen solution development in LCs is usually not provided. The reason for this could be that no static cell will be 100% sealed and dries out eventually during microscopy.

\* Arrows in Figure 3 would be helpful

We agree and have adjusted **Figure 4 (note that figure order has changed)** accordingly.

\* In Step 5, how does the program find and size the particles? It seems to fit all the particles to circles. Is that a valid assumption? Zooming in and showing the outline compared to the particle would be helpful to know how well it fits the particles

The algorithm **tracks the particles using TrackMate**. Indeed, TrackMate is searching for circular spots that might not properly reflect the particle size. The underlying algorithm is explained in great detail in the corresponding publication (Tinevez et al., 2017). This is why the **shape is analyzed in more detail by FIJI's Analyze Particles function**, where the **whole particle area is precisely measured** by integrating over the pixels that correspond to a



particle. The results of TrackMate and Analyze Particles are then combined using a script that compares the barycenter of the found spots with both methods. Only if the particle is cross-referenced by both methods, it will be regarded further.

To quantitatively analyze the size development of the particles, **the analysis follows the classic nucleation theory** developed by Wagner in 1961. There it is *lege artis* to define an **equivalent radius** that corresponds to a **sphere containing the volume the particle would have**. Classic nucleation theory is widely used in liquid cell microscopy (see for example Woehl et al. 2012 DOI: 10.1111/jmi.12508, Ngo et al 2015, Hutzler et al. 2018, Li et al 2018 DOI: 10.1007/s12274-018-2052-6) The circles drawn in the respective Figure correspond to this equivalent radius. They are not used to fit the particles and are shown for illustration only. **We do not want to state that the particles are spherical** in every case but use the equivalent radius to compare the size dynamics observed here between both, the particles detected here and experiments conducted by different groups. **Therefore, we honestly thank the reviewer for stressing this point, and have reformulated the respective paragraph:**

*In order to yield sufficient statistics, computational single particle tracking is required. By estimating the growth exponent  $\alpha$  of the **equivalent radius variation of individual particles** over time, information of the underlying reaction kinetics can be obtained. To do so, it is possible to introduce an equivalent radius based on the projected particle area, **even if not all particles are completely spherical** <sup>6,42</sup>*

\* What does "posterized images" mean? (Line 182)

The term means "binary". As this was not clear enough the term *posterized* was changed into *binary* in the manuscript:

*NOTE: This function requires binary images.*

## Reviewer #2:

### Manuscript Summary:

The protocol describes a method to make a graphene liquid cell based on a well etched in silicon nitride covered with a graphene sheet. Some exemplary results are included. This area of research is currently highly active and innovations in graphene liquid cells are needed. The topic of the paper thus certainly deserves publication. The scientific novelty is the accomplishment of this specific type of graphene liquid cell.

### Major Concerns:

1. I recommend including a schematic of the graphene liquid cell so that it becomes clear to the reader what type of graphene liquid cell is present here.

In addition to the detailed fabrication that was already visualized, we decided to reprint a three dimensional **GSMLC schematic** from Hutzler et al (2018). This is now **included as Figure 1**.

2. I recommend including a SEM image of a loaded and sealed well (or a few wells) to see if the graphene forms a flat coating with the well fully filled with liquid or if the graphene wrinkles inside the well. This is crucial information for the reader.

A representative **HAADF SEM image of a loaded GSMLC in STEM mode** at low acceleration voltage (29 kV) is displayed as **Figure 7**. It is clearly visible that the membrane shading stays mostly constant over the well region, but darkens towards the well center, which is illustrated in the Figure below, where intensity cross sections of the wells visible in Figure 7 are displayed (see **Figure A**).

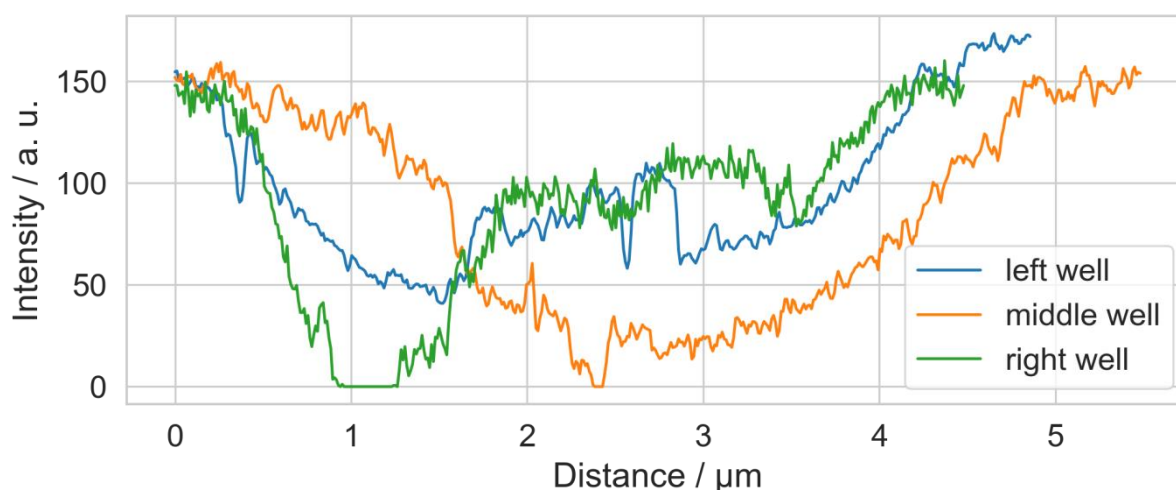


**Figure A:** Intensity cross section of the wells displayed in Figure 7 of the manuscript.

This accounts for **negative bulging**. This phenomenon is discussed with respect to analyses performed by Kelly et al.. They demonstrated that the negative bulging and (partial) well drying visible in **Figure 7** is directly **depending on the well diameter**. **Reducing the latter is therefore a feasible approach to homogenize the liquid thickness even further.**

3. A measurement or an estimate of the liquid thickness needs to be provided. Fig. 4 looks as if most liquid has disappeared. But nevertheless, thin liquid layer has remained such that

dynamics of nanoparticles, and dendrite growth can be observed. It is essential information for the reader to know exactly what kind of liquid configuration is obtained here.

Yes, the **liquid thickness is expected to be below 190 nm**. The shown SEM image (Figure 7 in the manuscript) supports this assumption. However, we observe **gas bubble formation** at the end of the provided supplementary video. Without liquid, this would be impossible. Also, dynamic processes such as the apparent **gold ion transport** to the supersaturated area of the dendrite growth are observed. This **contradicts with a negligible liquid thickness**. Based on these assumptions we expect a **liquid thickness between 50 and 100 nm**. However, as the utilized TEM does not support EELS or STEM-based liquid thickness measurements, we cannot provide a measurement for this dedicated experiment.

4. How is yield defined? I assume 75% refers to how many times one has to make a sample in order to obtain a workable device. But, how many well contain liquid in such a workable device?

Here, yield is defined as the **amount of successfully prepared GSMLC-frames, where sufficiently sealed wells for TEM investigations are present**. We added an explanatory comment to that statement in the manuscript:

*The redundant membrane windows, however, enhance the chances of preserving at least one membrane area. As a consequence, the yield (**amount of operable GSMLC chips**) achieved by a trained experimenter three out of four<sup>6</sup>, and thus exceeds the one achieved with graphene-based cells (25% – 50%)<sup>19</sup>.*

5. The authors should describe in detail what is meant by: "Also, the liquid loading is not trivial. It requires a dedicated training, similar to graphene cells." Is all detail included in the Jove protocol or if further training required?

Paragraph 4.5 of the protocol was adjusted to emphasize its importance:

*4.5 Carefully remove the TEM grid with a tweezer by pushing a tweezer tip between the grid and the GSMLC frame.*

*NOTE: Rash movements might break the underlying membrane. To reduce shear force damage, start from the grid site parallel to the smaller window edge.*

Still, without hands-on training the operation of a GSMLC will not be possible for reproducible measurement series.

### **Minor Concerns:**

1. Would it be possible to transfer the graphene without using a TEM grid?

In general, **it might be possible** to bypass the grid removal by transferring the graphene directly from the specimen solution. However, in this case, the supporting holey carbon membrane would be adjacent which is **expected to enhance the negative bulging** discussed in the paper.

2. The authors should discuss their liquid cell in relation to the system published by Kelly et al. What are advantages and disadvantages compared to that system?

Sealing prepatterned microwells with graphene on both, the bottom and top well site have been demonstrated before by both, Rasool et al (2016) on  $\text{Si}_3\text{N}_4$  wells and later Kelly et al. (2018) on h-BN-spacers. Applying two graphene membranes might **enhance the achievable resolution**; however a **two-fold graphene transfer would complicate the preparation process further** as this has proven to be the most sensitive preparation step. Furthermore, the above discussed **membrane bulging is expected to be even more critical in case of two graphene membranes**, because graphene is much more flexible than a  $\text{Si}_3\text{N}_4$  layer. In those architectures, the microwells were constructed using sequential focused ion beam (FIB) milling. Albeit this approach has proven to yield high-quality results in dedicated experiments, **FIB milling leads to a cumbersome and expensive cell production**. Utilizing single-shot patterning techniques that are already *lege artis* in today's semiconductor industry such as nanoimprint- or **photolithography, however, has the major advantage of fast, cheap and scalable mass production**.

Accordingly, the following paragraph was added to the discussion section of the manuscript:

*Sealing prepatterned microwells with graphene on both the bottom and top well site has been demonstrated before<sup>24,25</sup>. Applying two graphene membranes may enhance the achievable resolution. A twofold graphene transfer, however, would complicate the preparation process further; especially since this has proven to be the most sensitive preparation step (see below). Furthermore, the above discussed membrane bulging is expected to be even more critical in case of two graphene membranes, because graphene is much more flexible than a  $\text{Si}_3\text{N}_4$  layer. In those architectures, the microwells were constructed using sequential focused ion beam (FIB) milling. While this approach has proven to yield high-quality results, FIB milling is complicated and expensive cell production technique. Utilizing massively parallel single-shot patterning techniques that are already standard in today's semiconductor industry such as nanoimprint- or photolithography, however, has the major advantage of being fast, cheap and scalable for mass production.*

**Hutzler, Andreas**

---

**Von:** support@services.acs.org  
**Gesendet:** Montag, 4. März 2019 13:59  
**An:** Hutzler, Andreas  
**Betreff:** Regarding Incident 2589516 Permission request for reuse of one figure from article 10.1021/acs.nanolett.8b03388



Dear Dr. Hutzler,

Thank you for contacting ACS Publications Support.

Your permission requested is granted and there is no fee for this reuse.

In your planned reuse, you must cite the ACS article as the source, add this direct link

<<https://pubs.acs.org/doi/abs/10.1021/acs.nanolett.8b03388>>, and include a notice to readers that further permission related to the material excerpted should be directed to the ACS.

Please do not hesitate to contact us if you need any further assistance.

Best regards,

Ivan Ostojic  
ACS Publications  
Customer Services & Information  
Website: <https://help.acs.org>

***Incident Information:***


**Incident #:** 2589516  
**Date Created:** 2019-03-04T11:17:34  
**Priority:** 3  
**Customer:** Andreas Hutzler  
**Title:** Permission request for reuse of one figure from article 10.1021/acs.nanolett.8b03388  
**Description:** Hello,

We would like to reuse one figure (Figure 1) from the article <https://pubs.acs.org/doi/10.1021/acs.nanolett.8b03388> in a follow-up video article which will be published in the Journal of Visualized Experiments (<https://www.jove.com/journal>). This article describes technical details concerning the preparation of our liquid cells for electron microscopy schematics, which is depicted in this figure, was claimed to be shown by one of the reviewers. Therefore, we would like to use the figure with a reference to the original article instead of a newly designed schematics.

What do we have to do to get the permission for that?

Best regards,





Andreas Hutzler

---

Dr.-Ing. Andreas Hutzler

[andreas.hutzler@leb.eei.uni-erlangen.de](mailto:andreas.hutzler@leb.eei.uni-erlangen.de)

Tel.: 09131/85 28638

Electron Devices  
University of Erlangen-Nürnberg  
Cauerstraße 6  
91058 Erlangen

{CMI: MCID641546}

Dear Dr. Hutzler,

Thank you for contacting ACS Publications Support.

Your permission requested is granted and there is no fee for this reuse.

In your planned reuse, you must cite the ACS article as the source, add this direct link <https://pubs.acs.org/doi/abs/10.1021/acs.nanolett.8b03388>, and include a notice to readers that further permissions related to the material excerpted should be directed to the ACS.

Please do not hesitate to contact us if you need any further assistance.

Best regards,

Ivan Ostojic

ACS Publications

Customer Services & Information

Website: <https://help.acs.org>

Incident Information:

Incident #: 2589516

Date Created: 2019-03-04T11:17:34

Priority: 3

Customer: Andreas Hutzler

Title: Permission request for reuse of one figure from article 10.1021/acs.nanolett.8b03388

Description: Hello,

We would like to reuse one figure (Figure 1) from the article <https://pubs.acs.org/doi/10.1021/acs.nanolett.8b03388> in a follow-up video article which will be published in the Journal of Visualized Experiments (<https://www.jove.com/journal>). This article describes technical details concerning the preparation of our liquid cells for electron microscopy. The

schematics, which is depicted in this figure, was claimed to be shown by one of the reviewers. Thus, we would like to use the figure with a reference to the original article instead of a newly designed schematics.

What do we have to do to get the permission for that?

Best regards,

Andreas Hutzler

-----  
----

Dr.-Ing. Andreas Hutzler

[andreas.hutzler@leb.eei.uni-erlangen.de](mailto:andreas.hutzler@leb.eei.uni-erlangen.de)

Tel.: 09131/85 28638

Electron Devices

University of Erlangen-Nürnberg

Cauerstraße 6

91058 Erlangen